UNIVERSIDADE FEDERAL DO PARANÁ

MARINA SUTILLI

REGISTRO DA DEPOSIÇÃO TEMPORAL DE HIDROCARBONETOS EM TESTEMUNHOS SEDIMENTARES DAS ILHAS DECEPTION E PINGUIM (ANTÁRTICA)

PONTAL DO PARANÁ

2019

MARINA SUTILLI

REGISTRO DA DEPOSIÇÃO TEMPORAL DE HIDROCARBONETOS EM TESTEMUNHOS SEDIMENTARES DAS ILHAS DECEPTION E PINGUIM (ANTÁRTICA)

Dissertação apresentada como requisito parcial à obtenção do grau de Mestre em Sistemas Costeiros e Oceânicos, no Curso de Pós-graduação em Sistemas Costeiros e Oceânicos, Centro de Estudos do Mar, Universidade Federal do Paraná.

Orientador: Prof. Dr. César de Castro Martins

PONTAL DO PARANÁ

2019

CATALOGAÇÃO NA FONTE:
UFPR / SiBi - Biblioteca do Centro de Estudos do Mar
Liliam Maria Orquiza - CRB-9/712

Sutilli, Marina.
S966r Registro da deposição temporal de hidrocarbonetos em testemunhos sedimentares das ilhas Deception e Pinguim (Antártica). / Marina Sutilli. – Pontal do Paraná, 2019.
73 f.: il.; 29 cm.

Orientador: Prof. Dr. César de Castro Martins.

Dissertação (Mestrado) – Programa de Pós-Graduação em Sistemas Costeiros e Oceânicos, Centro de Estudos do Mar. Universidade Federal do Paraná.

1. Testemunhos sedimentares. 2. Depósitos de carvão. 3. Antártica. I. Martins, César de Castro. II. Universidade Federal do Paraná.

CDD 551.3

MINISTÉRIO DA EDUCAÇÃO
SETOR REITORIA
UNIVERSIDADE FEDERAL DO PARANÁ
PRÓ-REITORIA DE PESQUISA E PÓS-GRADUAÇÃO
PROGRAMA DE PÓS-GRADUAÇÃO SISTEMAS COSTEIROS
E OCEÂNICOS - 40001016054P6

TERMO DE APROVAÇÃO

Os membros da Banca Examinadora designada pelo Colegiado do Programa de Pós-Graduação em SISTEMAS COSTEIROS E OCEÂNICOS da Universidade Federal do Paraná foram convocados para realizar a arguição da dissertação de Mestrado de **MARINA SUTILLI** intitulada: **Registro da Deposição Temporal de Hidrocarbonetos em Testemunhos Sedimentares das Ilhas Deception e Pinguim (Antártica)**, após terem inquirido a aluna e realizado a avaliação do trabalho, são de parecer pela sua APROVADA no rito de defesa.

A outorga do título de mestre está sujeita à homologação pelo colegiado, ao atendimento de todas as indicações e correções solicitadas pela banca e ao pleno atendimento das demandas regimentais do Programa de Pós-Graduação.

Pontal do Paraná, 20 de Março de 2019.

CÉSAR DE CASTRO MARTINS
Presidente da Banca Examinadora (UFPR)

MARCIA CARUSO BICEGO
Avaliador Externo (USP)

RAFAEL ANDRE LOURENÇO
Avaliador Externo (USP)

AGRADECIMENTOS

A toda a minha família, especialmente para a minha mãe, Mari, pelo incentivo, compreensão e por acreditar que eu conseguiria.

Ao meu companheiro da vida, Joel Saalfeld, por todo o apoio que recebi nesses anos juntos, por acreditar em mim mais que eu mesma, e por sempre achar um jeito de me alegrar.

Ao meu orientador, Prof. Dr. César de Castro Martins, por mais dois anos de orientação e por todo o suporte, aprendizado e confiança que recebi. Obrigada por sempre incentivar os seus alunos a serem melhores!

Às melhores companheiras de laboratório, as LaGPoM girls: Ana Carol, Fer, Amanda, Ana Lúcia, Marina, Marines e Camila. Obrigada por toda a ajuda ao longo desses anos, por todas as risadas, cafés, e principalmente por tornarem o nosso ambiente de trabalho o melhor possível.

Aos amigos "pontalenses", em especial Iully, Isa, Tai, pela eterna amizade, por sempre terem um cantinho para me receber, e por saber que não existe tempo ruim com vocês.

Aos amigos que as montanhas colocaram no meu caminho: Dai, Anderson, Idce, Yara, por todos os perrengues, acampamentos e pelas nossas andanças na serra!

Aos colegas da turma de 2017 da PGSISCO, pelos bons momentos vividos durante esses anos de mestrado.

A todos os professores e demais funcionários do Centro de Estudos do Mar que contribuíram durante a minha formação.

À Coordenação de Aperfeiçoamento de Pessoal de Ensino Superior (CAPES) pela bolsa de mestrado.

"I believe that, with anything in life, if you have the patience, desire and passion, you can do whatever you set your mind to."

- Ed Viesturs

RESUMO

A distribuição vertical de hidrocarbonetos policíclicos aromáticos (HPAs) e hidrocarbonetos alifáticos (HAs), incluindo biomarcadores de petróleo (BMP), foi estudada em quatro testemunhos sedimentares coletados no entorno das Ilhas Deception e Pinguim, no Arquipélago Shetlands do Sul, Antártica. As concentrações de HPAs totais nas amostras da Ilha Deception variaram de 2,01 a 26,84 ng g^{-1} e na Ilha Pinguim de 13,20 a 60,34 ng g^{-1}. As fontes de HPAs nas amostras da Ilha Deception foram multiplas, com predominância de origem petrogênica nos últimos 10 anos. Na Ilha Pinguim, os HPAs foram associados a um predomínio de fontes petrogênicas, e também relacionadas às contribuições naturais proveniente da erosão de depósitos de carvão. Os valores de AHs totais nas amostras da Ilha Deception variaram de 4,50 a 19,01 µg g^{-1}, e na Ilha Pinguin de 5,35 a 21,91 µg g^{-1}. Na Ilha Deception, o padrão de distribuição de *n*-alcanos sugeriu a presença de resíduos de petróleo nas seções de topo. Na Ilha Pinguim, a principal fonte de *n*-alcanos foi de aporte marinho. Na Ilha Deception, terpanos e hopanos foram detectados, relacionados ao uso de combustíveis fósseis para a geração de energia e para os diferentes tipos de embarcações. Na Ilha Pinguim, apenas os terpanos foram detectados, associados à erosão de depósitos de carvão. O leve aumento nos níveis de hidrocarbonetos observado a partir de 1980 na Ilha Deception foi relacionado ao desenvolvimento do turismo na região e ao estabelecimento de estações científicas. Na Ilha Pinguim, foram detectados hidrocarbonetos de origem antrópica nas seções recentes, podendo ser relacionados ao desenvolvimento do turismo próximo à ilha, atividades científicas pontuais e ao aumento do tráfego de embarcações na região. Em geral, a concentração de hidrocarbonetos encontrada em ambas as ilhas foi comparada àquelas encontradas em regiões antárticas não contaminadas.

Palavras-chave: Testemunhos sedimentares. Depósitos de carvão. Antártica.

ABSTRACT

The vertical distribution of polycyclic aromatic hydrocarbons (PAHs) and aliphatic hydrocarbons (AHs), including petroleum biomarkers (PBMs), was studied in four sediment cores collected around Deception and Penguin Island, Antarctica. Total PAHs concentrations in Deception Island samples ranged from 2.01 to 26.84 ng g^{-1}, whereas levels from Penguin Island varied between 13.20 and 60.34 ng g^{-1}. Multiple sources of PAHs were verified in Deception Island, with petrogenic-derived compounds being predominant over the last 10 years. In Penguin Island, PAHs with a petrogenic source pattern were observed, being related to natural contributions from the erosion of coal deposits. Total AHs in Deception Island ranged from 4.50 to 19.01 µg g^{-1}, whereas those in Penguin Island varied between 5.35 and 21.91 µg g^{-1}. In Deception Island, the *n*-alkanes distribution pattern showed the presence of petroleum residues in the top sections. In Penguin Island, the main source of *n*-alkanes was marine inputs. In Deception Island, both terpanes and hopanes were detected, related to the use of fossil fuels for power generation and in different types of vessels. In Penguin Island, only terpanes were detected, associated with the erosion of coal deposits. The slight increase in hydrocarbon levels observed from 1980 onward in Deception Island was assumed to be due to the development of tourism in the region and to the scientific station activities. In Penguin Island, anthropogenic-related hydrocarbons were detected in the recent sections and were linked to the development of tourism near the island, scientific activities and the increase in vessel traffic. In general, the concentrations of hydrocarbons found around both islands were compared to those found in uncontaminated Antarctic regions.

Key-words: Sediment core. Coal deposits. Antarctica.

SUMÁRIO

1. Contextualização geral

A Antártica já foi reconhecida como a última região intocada pelas perturbações humanas, porém, as atividades antrópicas desenvolvidas neste continente principalmente a partir de 1900 causaram diversos tipos de impactos, como a introdução de espécies invasoras, através da água de lastro dos navios, depleção de estoques pesqueiros devido à pesca excessiva, contaminação por compostos inorgânicos e orgânicos, entre outros (Bargagli et al., 2008; Aronson et al., 2011).

Nas últimas três décadas, diversos estudos relatam o aumento da introdução e acumulação de contaminantes na Antártica, estando os hidrocarbonetos, principalmente os policíclicos aromáticos, entre as maiores classes emitidas (Cincinelli et al., 2008). As atividades relacionadas às estações científicas (instaladas principalmente a partir de 1950), ao turismo (estabelecido a partir de 1960) e ao tráfego de embarcações são listadas como as principais fontes de introdução desses compostos para o ambiente Antártico (Curtosi et al., 2007; Aronson et al., 2011).

Os hidrocarbonetos policíclicos aromáticos (HPAs) são comumente abordados em estudos de avaliação ambiental, uma vez que são considerados tóxicos ao ambiente marinho e à saúde de organismos (Zhang et al., 2008). Além dos HPAs, hidrocarbonetos alifáticos (HAs) podem ser utilizados para auxiliar na identificação da contaminação por petróleo em um ambiente, bem como de possíveis contribuições naturais de hidrocarbonetos, associadas a fontes biogênicas (Readman et al., 2002; Tolosa et al., 2004).

Em uma região de características peculiares, onde a biodiversidade é única e consequentemente mais vulnerável aos efeitos adversos de contaminantes, estudos ambientais devem ser realizados com frequência, a fim de diagnosticar e até mesmo evitar impactos irreversíveis. Nesse contexto, tendo em vista a importância global do continente Antártico, estudos utilizando marcadores geoquímicos são extremamente

necessários, pois possibilitam compreender a dinâmica do ambiente e alterações significativas ao longo dos anos.

A presente dissertação de Mestrado pretende auxiliar no levantamento de dados sobre hidrocarbonetos em sedimentos do entorno das Ilhas Deception e Pinguim, por meio da construção de registros históricos da introdução desses compostos e do estabelecimento da relação entre eles e as atividades humanas desenvolvidas na região, possibilitando um maior entendimento de como as ações antrópicas estão influenciando regiões da Antártica. A fim de uma maior caracterização quanto à introdução de hidrocarbonetos na região, incluímos no estudo a determinação dos HAs (abordando também os biomarcadores do petróleo) e os HPAs. Portanto, os objetivos do presente estudo são:

1.1 Objetivo geral

- Estudar a distribuição vertical de hidrocarbonetos em testemunhos sedimentares previamente datados das Ilhas Deception e Pinguim, regiões antárticas sujeitas a alterações ambientais provenientes de atividades antrópicas e de processos naturais;

1.2 Objetivos específicos

- Determinar a concentração de diferentes classes de hidrocarbonetos (hidrocarbonetos policíclicos aromáticos e hidrocarbonetos alifáticos: como *n*-alcanos, pristano, fitano e biomarcadores do petróleo);

- Identificar quais as principais fontes dessas classes de hidrocarbonetos e avaliar se existe contaminação nas regiões estudadas;

- Associar a variação das concentrações dos hidrocarbonetos na coluna sedimentar com os eventos históricos e características específicas de cada local.

2. Manuscrito

Registro da deposição temporal de hidrocarbonetos em testemunhos sedimentares das ilhas Deception e Pinguim (Antártica)

Depositional input of hydrocarbons recorded in sedimentary cores from Deception Island and Penguin Island (Antarctica)

Revista pretendida: *Environmental Pollution* (Qualis A1, IF = 4.358)

* Marina Sutilli [1,2], Paulo A. L. Ferreira [3], Rubens C. L. Figueira [3], [$] César C. Martins [2]

[1] Programa de Pós-Graduação em Sistemas Costeiros e Oceânicos (PGSISCO), Universidade Federal do Paraná, Caixa Postal 61, 83255-976, Pontal do Paraná, PR, Brazil.

[3] Centro de Estudos do Mar, Universidade Federal do Paraná, Caixa Postal 61, 83255-976, Pontal do Paraná, PR, Brazil.

[2] Instituto Oceanográfico da Universidade de São Paulo, Praça do Oceanográfico, 191, 05508- 900, São Paulo, SP, Brazil.

Corresponding authors:

E-mail addresses: * marinasutilli@gmail.com (M. Sutilli)

[$] ccmart@ufpr.br (C.C. Martins)

2.1 Introduction

Despite the scarce human presence on the Antarctic continent, several studies have reported an increased accumulation of a variety of contaminants over recent decades, showing the impact of anthropic activities in the region (Bargagli et al., 2008; Aronson et al., 2011). Activities related to scientific stations (established mainly since 1950), tourism (started in approximately 1960), vessel traffic and the long-range transport of persistent organic pollutants are known as main sources for the input of contaminants in the Antarctic environment (Curtosi et al., 2007; Aronson et al., 2011)

Polycyclic aromatic hydrocarbons (PAHs) are one of the most significant groups of contaminants found in Antarctica (Bengtson, 2010; Cincinelli et al., 2008). They are primarily associated with petroleum and its derivates, being widely employed as markers of anthropogenic activities. Sources of PAHs to Antarctica include sewage discharges, garbage incineration, burning of fossil fuels, accidents involving large and small oil spills that can occur in operational activities involving all types of vessels (ships and support boats) (Negri et al., 2006; Curtosi et al., 2007; Dauner et al., 2015).

Aliphatic hydrocarbons (AHs) include *n*-alkanes, isoprenoids (such as pristane and phytane), and petroleum biomarkers (such as terpanes and hopanes). Their analysis can be used as a tool to distinguish anthropogenic from natural sources of hydrocarbons, since they have different carbon and chemical structural signatures for each origin (Aboul-Kassim and Simoneit, 1996). In general, the distribution of *n*-alkanes of anthropic origin is marked by the non-predominance of compounds with odd or even carbon chains, whereas the distribution in natural sources has a marked presence of odd carbon chains (Volkman et al., 1992). However, some authors noticed that marine organism from Antarctica can exhibit a different distribution pattern, with the predominance of even carbon chains or without an odd/even predominance (Venkatesan and Kaplan, 1987; Cripps, 1989; Martins et al., 2004). Petroleum biomarkers (PBMs) have

been used to identify and provide more accurate information from the type and source of petroleum and by-products in marine sediments, since the distribution of the compounds can be different from oil to oil (Wang et al., 1999).

The South Shetland Islands (SSI, Fig. 1) are one of the most easily accessible regions of Antarctica, mainly due to its proximity to South America, which provides more favourable conditions for the establishment of scientific stations and the development of tourism. Deception Island and Penguin Island, located in the SSI, have been designated as Antarctic Specially Protected Areas (ASPA) (Guerra et al., 2011) and comprise areas largely targeted by tourism expeditions, due to their great scenic beauty, unusual landscapes and wild life (Pfeiffer and Peter, 2004; Dibbern, 2010).

The aim of the present study is to determine the concentrations and the vertical distribution of PAHs, AHs and PBMs in sedimentary cores from Deception and Penguin Island, as well as to assess the main sources of these compounds and associate their levels with historical events and local characteristics of the studied region. Despite the recent history of human activities in these regions, a comprehensive study on hydrocarbons has not been carried out in the marine sediment cores of both islands.

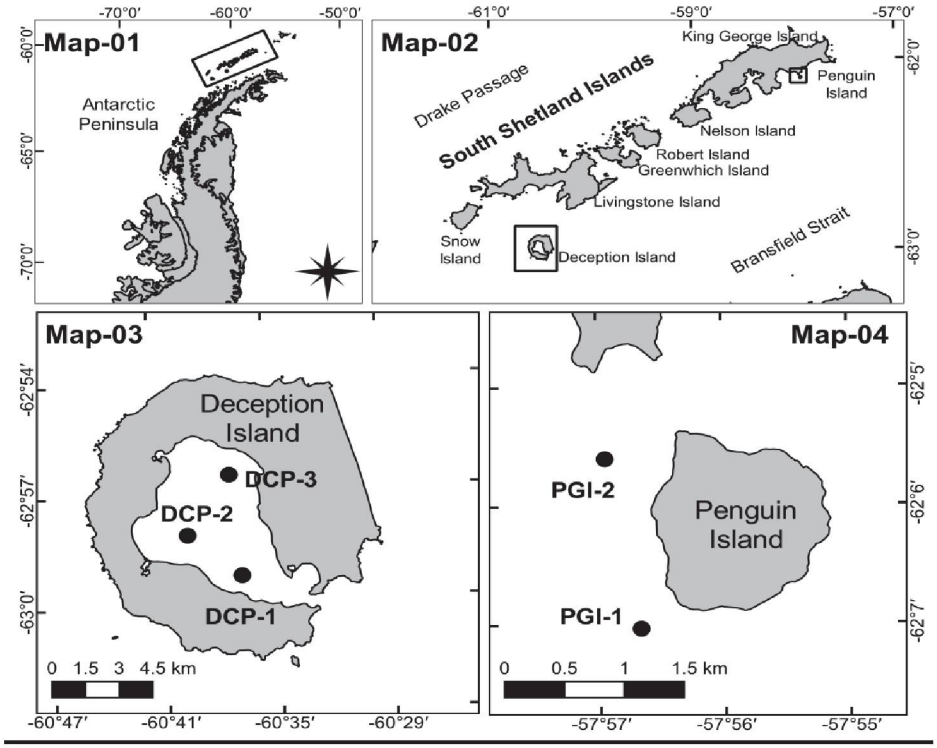

Fig. 1. Map of the study area showing: Antarctic Peninsula (Map 01), South Shetland Islands (Map 02) and sampling locations (Map 03 - Deception Island, DCP-1 and DCP-2 cores, surficial sediment DCP-3; Map 04 - Penguin Island, PGI-1 and PGI-2 cores).

2.2 Study area

2.2.1 Deception Island

Deception Island (62°57'S, 60°38'W, Fig. 1, Map-03) is a volcanic and partially submerged island (Smellie, 2001). The submerged portion consists of a semi-enclosed caldera known as Port Foster (Flexas et al., 2017). Regular volcanic activity occurs in the islands, and the last volcanic eruptions occurred in 1967, 1969 and 1970 (Baker et al., 1975; Smith Jr. et al., 2003).

Deception Island has historically been considered the 'commercial' centre of Antarctica (Dibbern, 2010). Between 1910 and 1931, a Norwegian whaling station was built and operated at Whalers Bay (Smith Jr et al., 2003). However, with the decline in whale stocks, the whaling station was deactivated, and in 1944, the building was transformed by the

British Antarctic Survey into a scientific station (Smith Jr et al., 2003). In the following years, two other countries established scientific stations on the island: Argentina (built in 1948) and Chile (built in 1955). The Chilean and British stations were partly buried by the eruption in 1969 (Smith Jr et al., 2003). Currently, there are two scientific stations on the island, the Argentinian "Decepción" and the Spanish "Gabriel de Castilla" (founded in 1990), located on the margins of Fumarole Bay. In the late 1950s, tourism began to develop, and Deception Island became one of the most visited sites in Antarctica (Dibbern, 2010).

2.2.2 Penguin Island

Penguin Island (62°06'S, 57°54'W, Fig. 1, Map-04) is an inactive volcano located on the southeast side of King George Island (Pfeifer and Peter, 2004; Ceschim et al., 2016). The island is frequently visited by tourists due to the high diversity of species, great scenic value and traces of whale fishing (such as bones and harpoons) (Pfeiffer and Peter, 2004; Guerra et al., 2011). Although no scientific stations are placed on the island, it is located near King George Island, where many research stations are located, leading to an impact of the continuous presence of research activities on this environment, especially by an atmospheric-derived compounds contribution, since wind directions to northwest and north are not uncommon in the region (Braun et al., 2001; Ferron et al., 2004). The area is extremely sensitive to potential environmental impacts due to its easy access, its diversity of flora and fauna and, and especially, for being a breeding ground and birds nesting area.

2.3 Material and Methods

2.3.1 Sediment sampling

Four short sediment cores (length ranging from 7 to 18 cm) were taken during the 2007-2008 austral summer, using a mini-box core sampler (25x25x55 cm). Cores were subsampled to 1-2 cm, placed in

aluminium containers and stored at -20 °C for further analysis (Ceschim et al., 2016). In Deception Island, cores were collected near the Netuno volcano (DCP-1, 62°59.50'S, 60°37.40'W) and Fumarole Bay (DCP-2, 63º58.30'S, 60º40.20'W) at a water depth of approximately 90 m. A superficial sediment sample was also collected in the region (DCP-3). In Penguin Island, the samples were obtained from a water depth of 20-30 m. PGI-1 core was collected from the south of the island, 500 m offshore from the penguin colonies (62°06'S, 58°05'W), whereas PGI-2 was sampled in the west, across from King George Bay (62°02'S, 58°02'W).

2.3.2 Dating of cores

For the determination of the recent sedimentation rate and core estimated dating, the ^{210}Pb activity was measurement based on gamma-ray spectrometry using a hyperpure Ge detector (model GEM60190; EGG&ORTEC) (Ceschim et al., 2016). Sedimentation rate estimates were based on the concentration initial constant (CIC) model described by Robbins and Edgington (1975). The instrumental procedures and quality assurances was fully described in (Combi et al., 2013). The average sedimentation rate obtained was 0.091 ± 0.004 cm yr^{-1} for PGI-1, 0.251 ± 0.010 cm yr^{-1} for PGI-2, 0.212 ± 0,013 cm yr^{-1} for DCP-1 and 0.167 ± 0.011 cm yr^{-1} for DCP-2. A period of 176 years (1831 to 2007), 72 years (1935 to 2007), 47 years (1960 to 2007) and 60 years (1947 to 2007) was estimated for PGI-1, PGI-2, DCP-1 and DCP-2, respectively.

2.3.3 Hydrocarbons analysis

Prior to the analytical method, the samples were oven-dried at 40 °C for two days, macerated with mortar and pestle and stored in glass bottles. The procedures for sediment analysis were based on Wisnieski et al. (2016).

Approximately 15 g of dry-weight sediment was Soxhlet extracted for 8 h with 80 mL of a *n*-hexane and dichloromethane (DCM) mixture (1:1,

v/v), copper pieces (for the removal of inorganic sulphur), boiling spheres and 100 µL of a surrogate standards mixture containing 1-hexadecene and 1-eicosene (25 ng μL^{-1}) for AHs, naphthalene-d_8, acenaphthen-d_{10}, phenanthrene-d_{10}, chrysene-d_{12} and perylene-d_{12} (2.5 ng μL^{-1}) for PAHs, and 5α-cholestane-d_4 (2.5 ng μL^{-1}) for PBMs. The extract was reduced to 2 mL using rotary evaporation and submitted to a clean-up procedure using a column containing 3.2 g of silica, 1.8 g of alumina (both 5% deactivated) and sodium sulphate. The column was first eluted with 10 mL of *n*-hexane, removing the first fraction (AHs and PBMs), and then eluted with 15 mL of a DCM and *n*-hexane mixture (3:7, v/v), removing the second fraction (PAHs). Subsequently, the obtained fractions were concentrated by rotary evaporation and transferred to calibrated glass vials with a final volume of 500 µL. Before the instrumental analysis, an internal standards mixture was added to the final extract of each sample, containing 100 µL of benzo[*b*]fluoranthene-d_{12} (2.5 ng μL^{-1}) for PAHs, 1-tetradecene (25 ng μL^{-1}) for AHs and pregnane-d_4 (2.5 ng μL^{-1}) for PBMs.

Instrumental analysis for AHs was performed with an Agilent GC 7890A gas chromatography (GC) instrument equipped with a flame ionization detector and an Agilent 19091J-413 capillary fused-silica column coated with 5% diphenyl/dimethylsiloxane (30 m length, 0.32 mm ID, 0.25 µm film thickness). Hydrogen was used as the carrier gas. About 2 µL of each sample was injected in splitless mode. The injector temperature was 280 ºC and the temperature of the GC oven was programmed as follows: 40 - 60 ºC at 20 ºC min^{-1}, then 60 - 290 ºC at 5 ºC min^{-1}, and finally 290 - 300 ºC at 5 ºC min^{-1}. The compounds were identified using the HP Chemstation program (G2070 BA), by matching the retention time to the results from the standard mixtures of *n*-alkanes (C_{10} - C_{40}) and isoprenoids (DRH-008S-R2, AccuStandard, USA). The levels were obtained by using the internal standard peak area and response factor method and a calibration curve for individual compounds (0.25 - 10.0 ng μL^{-1}, $r > 0.995$).

The instrumental analysis for PAHs and PBMs was performed with an Agilent CG 7890A GC instrument coupled with a mass spectrometer

(Agilent 5975C inert MSD with Triple-Axis Detector). The column used was an Agilent 19091J-433 capillary fused-silica column coated with 5% diphenyl/dimethylsiloxane (30 m length, 0.25 mm ID, 0.25 µm film thickness). The oven heating program used was similar to those adopted for AHs. Helium was used as the carrier gas. The data were obtained using SIM (Selected Ion Monitoring) mode, and the quantification was based on the integration of specific fragment ion (m/z) peaks area using an Agilent Enhanced Chemstation (G1701 CA) program. The PAHs were identified by matching the retention time with the results obtained from the standard mixtures (Z-014G-FL, AccuStandard, USA), and with a calibration curve ranging from 0.10 to 2.00 ng μL^{-1}. PBMs were quantified based on response factor of 17α(H),21β(H)-Hopane-C_{30}-αβ and 5α-cholestane-C_{27}-ααα-20R (both from Chiron) with same concentrations range that PAHs, and identified by their m/z compared to m/z chromatograms obtained in the literature (Wang et al., 2009; Tolosa et al., 2009; Yang et al., 2011) and from injected oil samples (Arab Light, MF 380 and Marlim Blend). The complete list of organic compounds analyzed is presented as Supplementary Data (Tables S1 - S3).

2.3.4 Quality assurance procedures

Quality assurance was based on blanks extraction (which consist in 15 g of sodium sulfate) and the recoveries of surrogates standard. Procedural blanks were taken for each group of eleven samples and when necessary (*e.g.* values above 3 times de detection limits), the values found in the blanks were discounted from the samples. The mean surrogate recoveries in the extracted samples were 43 ± 25 % for naphthalene-d_8, 54 ± 29 % for acenapthene-d_{10}, 73 ± 26 % for phenanthrene-d_{10}, 79 ± 13 % for chrysene-d_{12}, 71 ± 25 % for perylene-d_{12}, 67 ± 8 % for 1-hexadecene, 95 ± 8 % for 1-eicosene and 98 ± 34 % for 5α-cholestane-d_4. Surrogate recoveries in the samples were in the acceptable range of recuperation (40 - 120%) for at least 80% of samples analyzed, considering all classes of hydrocarbons.

The instrumental detection limits named as detection limits (DL) was adopted in this study and were 0.001 μg g^{-1} for the *n*-alkanes and 0.50 ng g^{-1} for the PAHs and PBMs. These data are based on the lowest sensitive of PAHs and *n*-alkanes concentration (0.02 and 0.04 ng μL^{-1}, respectively) multiplied by the final extracted volume (500 μL) and divided by the weight sediment (20 g) before extraction.

In addition, the method accuracy was checked by the extraction of three replicates of standard reference material (SRM) for sediment from the IAEA (International Atomic Energy Agency, IAEA408, Vienna, 1999). The results were within the upper and lower 95% confidence interval reference values for 81% of PAHs. Results of procedural blanks and SRM can be found in Supplementary Data (Tables S1 - S3).

2.3.5 Data analysis

The studied area map was generated on the software Q.GIS (version 2.18.22). Statistical analyses (Spearman correlations and principal component analysis - PCA) were performed through the software R Studio (version 0.98.1103). Prior to the PCA, the variables studied were normalized (values were subtracted from the mean and divided by the standard deviation). Additional parameters such as grain size distribution (Fig. S1) and chlorophyll-*a* were used in this study to perform correlations with our data. These data were obtained by Ceschim et al. (2016) and Ceschim (2010), where a detailed description from each parameter can be found.

2.4 Results and Discussion

2.4.1 Hydrocarbons levels

Vertical distribution of total PAHs (∑PAHs, except perylene levels, due to its natural contribution as the principal source) in sediment cores from Deception and Penguin Island are shown in Fig. 2. Sum parameters and ratios results are summarized in Tables S4-S7. ∑PAHs in Deception Island varied between 7.68 to 26.84 ng g^{-1} in DCP-1 (average =14.23 ±

6.44 ng g^{-1}) and from 2.01 to 19.57 ng g^{-1} (average = 10.84 ± 6.05 ng g^{-1}) in DCP-2. In DCP-3 (surficial sediment), ∑PAHs was detected in trace amounts (3.75 ng g^{-1}). In Penguin Island, ∑PAHs varied from 13.20 to 55.99 ng g^{-1} (average= 22.65 ± 12.61 ng g^{-1}) in PGI-1 and from 23.28 to 60.34 ng g^{-1} (average = 35.32 ± 8.53 ng g^{-1}) in PGI-2 cores.

Concentrations of PAHs detected in Deception and Penguin Island were in the same range as those found in Ardley and Nelson Islands (7.33 - 13.64 and 15.32 - 33.79 ng g^{-1}, respectively) (Dauner et al., 2015), Prydz Bay (12.95 - 30.93 ng g^{-1}) (Xue et al., 2016) and Ross Sea (8 - 54 ng g^{-1}) (Venkatesan, 1988a). The levels found in these areas do not indicate contamination by PAHs and in specific cases were associated with natural origin. Our levels were low compared to regions where some punctual contamination has been expected due human activities, such as Fields Peninsula (0.54 - 228.2 ng g^{-1}) (Prendéz et al., 2001), Potter Cove (7.33 - 210.02 ng g^{-1}) (Dauner et al., 2015) and Admiralty Bay (9.45 - 270.5 ng g^{-1}) (Martins et al., 2004). Finally, the levels were much lower than those observed in the region close to McMurdo Sound station, where a pronounced history of anthropogenic hydrocarbon input has been found (levels in the range of 270 to 5,024 ng g^{-1}) (Kim et al., 2006; Negri et al., 2006).

Vertical distribution of total aliphatic hydrocarbons (ΣAHs) in Deception and Penguin Island are shown in Fig. 3. Sum parameters and diagnostic ratios are summarized in Tables S4-S7. ΣAHs in Deception Island varied between 6.27 - 19.01 µg g^{-1} (average= 11.13 ± 4.36 µg g^{-1}) in DCP-1 and from 4.50 - 8.67 µg g^{-1} (average= 6.61 ± 1.36 µg g^{-1}) in DCP-2. In DCP-3, value of ΣAHs found was 4.63 µg g^{-1}. In Penguin Island, the levels were in the range between 5.35 to 13.39 µg g^{-1} (average= 8.66 ± 2.20 µg g^{-1}) in PGI-1 and from 5.57 to 21.91 µg g^{-1} (average= 9.05 ± 3.92 µg g^{-1}) in PGI-2.

ΣAHs values in this study were far below the threshold level of 100 µg g^{-1}, which suggests oil contamination in marine environments (Volkman et al., 1992). On average, the values found in this study were similar to those reported for Admiralty Bay (0.15 - 13.1 µg g^{-1}) (Martins et al., 2004)

306 and Davis Bay (0.25 - 9.0 μg g^{-1}) (Green and Nichols, 1995), higher than
307 those observed in Potter Cove (0.52 - 4.94 μg g^{-1}) (Dauner et al., 2015),
308 and lower compared to the region of McMurdo Sound (4,500 μg g^{-1})
309 (Lenihan et al., 1990), which is considered highly contaminated.

310 The unresolved complex mixture (UCM), defined as a group of
311 alicyclic and branched hydrocarbons that cannot be resolved by the
312 traditional chromatographic techniques (Bouloubassi and Saliot, 1993),
313 was observed in all samples (Fig. 3), with averages of 7.10 ± 2.55 μg g^{-1} in
314 DCP-1; 4.02 ± 1.21 μg g^{-1} in DCP-2; 4.37 ± 0.71 μg g^{-1} in PGI-1 and 3.84 ±
315 2.05 μg g^{-1} in PGI-2. UCM concentrations <10 μg g^{-1} are usually related to
316 weathering of ancient rocks and bacterial reworking of sedimentary
317 organic matter (Volkman et al., 1992), indicating a predominant natural
318 organic matter input for both islands. Total *n*-alkanes (*n*-alks, $\sum n\text{-}C_{10}$ to *n*-
319 C_{40}, Fig. 3) ranged from 0.31 to 2.48 μg g^{-1} in Deception Island, with similar
320 levels in both cores. In Penguin Island, the values of *n*-alks varied from
321 0.43 to 2.22 μg g^{-1}, with no significant variations between the cores.

322 Total terpanes in Deception Island varied between 1.48 to 7.14 ng
323 g^{-1} (average= 4.68 ± 1.74 ng g^{-1}) in DCP-1 and from 12.48 to 35.45 ng g^{-1}
324 in DCP-2 (average = 25.92 ± 10.34 ng g^{-1}). In DCP-3, terpanes were
325 detected in trace amounts (0.65 ng g^{-1}). In Penguin Island, values of total
326 terpanes were found in the range of <DL to 32.60 ng g^{-1} (average= 8.31 ±
327 8.40 ng g^{-1}) in PGI-1 and from < DL to 15 ng g^{-1} (average = 5.81 ± 4.93 ng
328 g^{-1}) in PGI-2. The values of total terpanes found in this study are
329 comparable to data reported in cores collected in a pristine region, Hecate
330 Strait, in the Pacific Ocean (1.0 to 15 ng g^{-1}) (Yunker et al., 2014) and with
331 values observed in surficial sediments of the Arctic Ocean (2.4 to 74 ng g^{-1})
332 (Yunker et al., 2011).

333 Total hopanes were detected in the range of <DL to 8.47 (average
334 = 1.37 ± 2.81 ng g^{-1}) in DCP-1 and from 4.32 to 22.10 ng g^{-1} (average =
335 12.35 ± 5.38 ng g^{-1}) in DCP-2. Values of hopanes in Deception Island
336 were lower compared with those found in some regions of the Arctic
337 Ocean (levels reaching 800 ng g^{-1}; Yunker et al., 2011). Hopanes were
338 detected neither in sediment cores from Penguin Island nor in DCP-3.

339

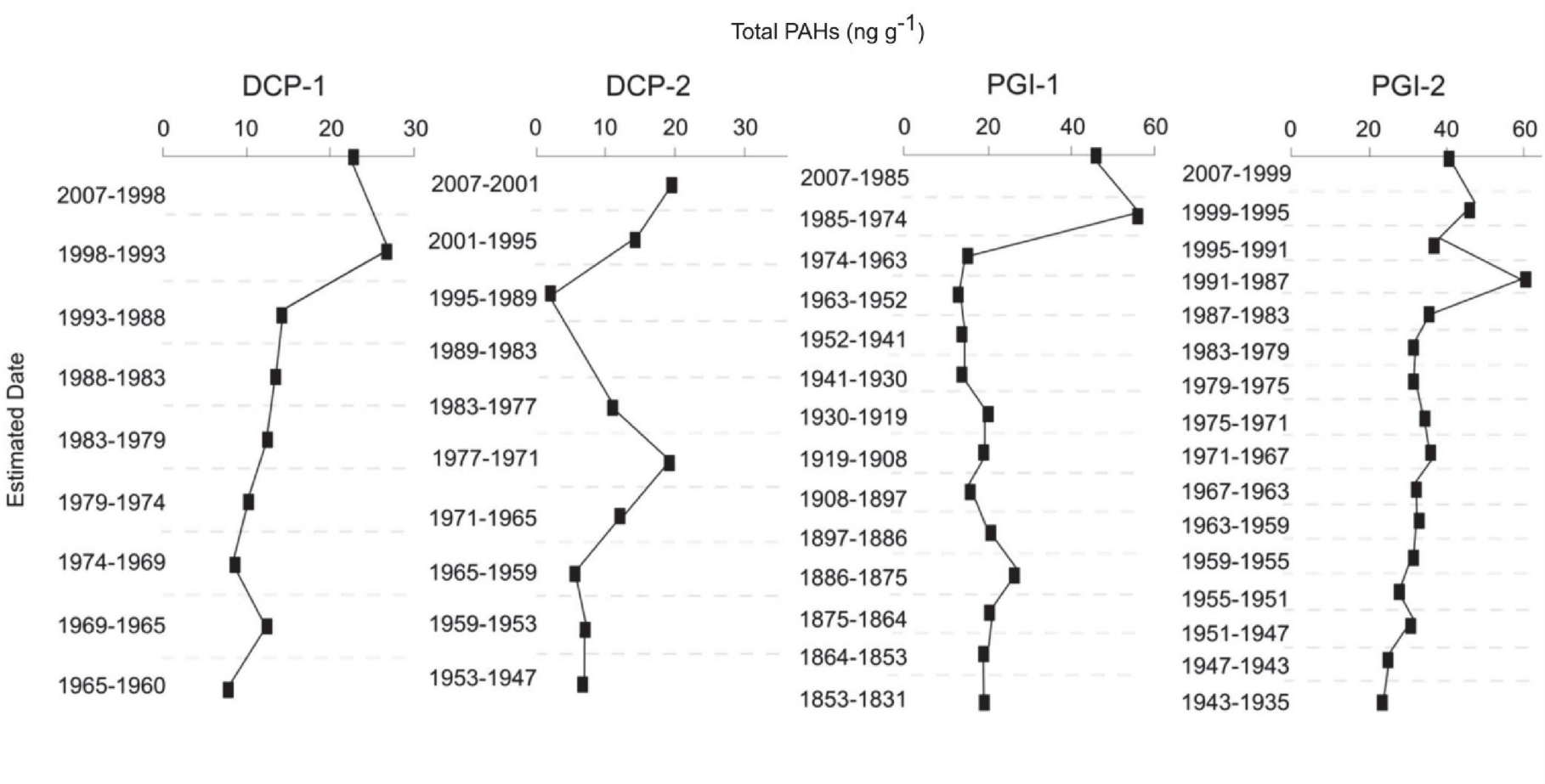

340

341 Fig. 2. Total PAHs (in ng g^{-1}) in sediment cores from DCP-1, DCP2, PGI-1 and PGI-2.

342

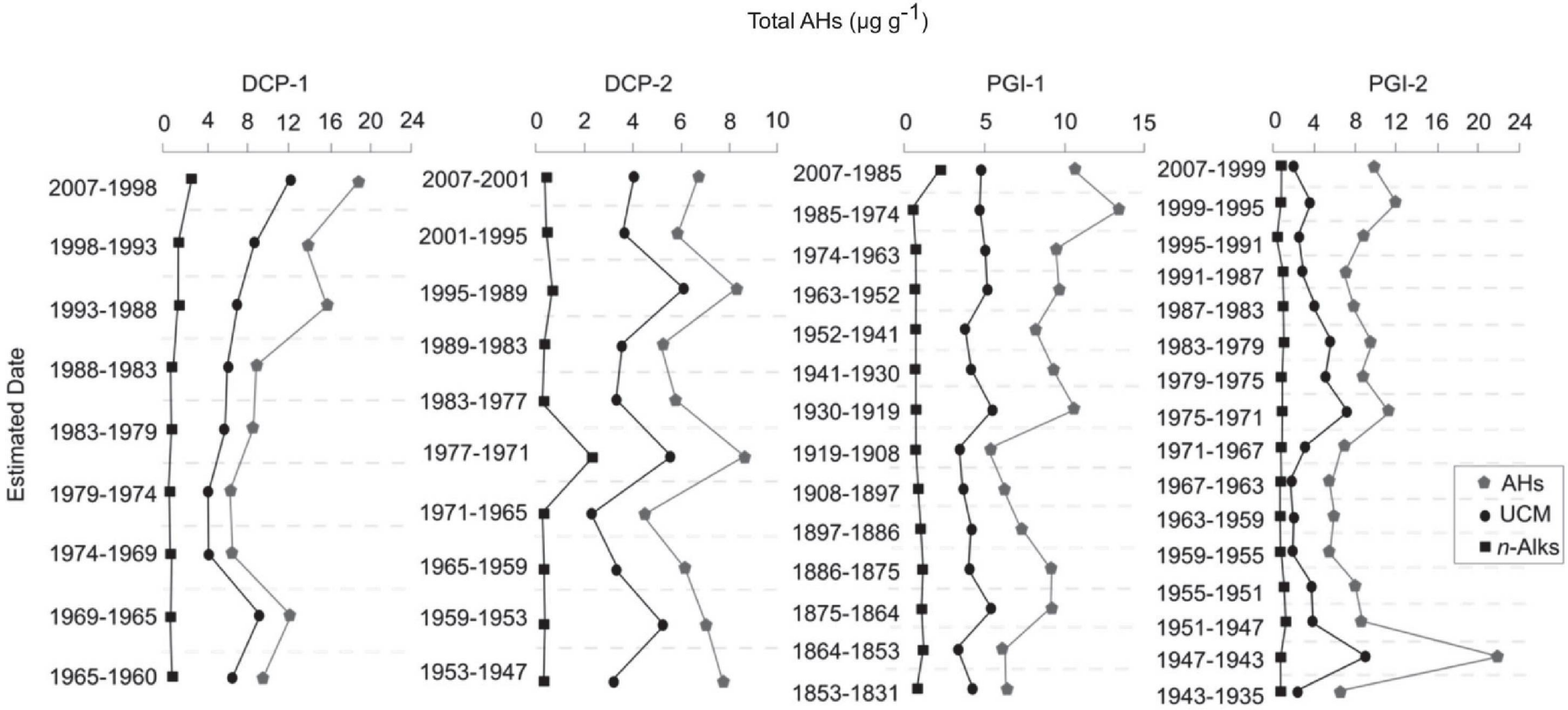

343

344 Fig. 3. Total AHs, *n*-alks and UCM (in μg g^{-1}) in sediment cores from DCP-1, DCP-2, PGI-1 and PGI-2

345

346 *2.4.2 Hydrocarbons distribution and sources*

347

348 The mean distribution of individual PAHs in Deception Island is
349 presented in Fig. 4A. Concentration profiles for total alkylated PAHs
350 (alkyl), 2-3-ringed PAHs, and 4-6-ringed PAHs can be found in Fig. S2.
351 Alkyl-naphthalenes (C_2 and C_3, respectively) had the highest relative
352 concentrations in DCP-1 (alkyl PAHs represented 61.4% of ∑PAHs). In
353 DCP-2 core, C_2-fluorene had the highest levels, followed by alkyl-
354 naphthalenes (C_2 and C_3, respectively, and alkyl PAHs represented 65.9%
355 of ∑PAHs). In DCP-3, only alkyl compounds were found, with C_2-
356 napththalene being predominant (0.93 ng g^{-1}). The individual PAH
357 distribution patterns observed in both cores and in DCP-3 were similar,
358 suggesting the presence of petroleum residues, probably derived from the
359 operations of scientific stations and vessel traffic in the region.

360 The mean distribution of individual PAHs in Penguin Island is
361 presented in Fig. 4B. The concentration profiles for alkyl, 2-3-ringed and 4-
362 6-ringed PAHs are shown in Fig. S2. Perylene had the highest values in
363 PGI-1, followed by C_2 and C_3 naphthalene. Alkyl PAHs varied from 6.76 to
364 17.20 ng g^{-1} (average = 11.78 ± 3.10 ng g^{-1}) representing 52.0% of
365 ∑PAHs, being predominant in almost the entire core represented. In the
366 recent sections of PGI-1 (1974-2007), a predominance of 4-6-ringed
367 compounds was observed. In PGI-2 core, alkyl-naphthalenes (C_2, C_1 and
368 C_3, respectively) had the highest levels. Alkyl PAHs in PGI-2 ranged from
369 20.29 to 53.20 ng g^{-1} (average = 27.48 ± 7.77 ng g^{-1}), corresponding to
370 77.7% of ∑PAHs, being predominant in the entire core.

371 The PAH distribution found in Penguin Island had a "petrogenic
372 pattern" in both cores, due the predominance of alkyl PAHs. However, the
373 levels (especially those observed in the deeper sections) can be related to
374 constant natural inputs. The PAH compositions found in PGI-1 and in PGI-
375 2 were quite similar to those found in coal samples, as coal contains large
376 amounts of PAHs, and a predominance of naphthalene, phenanthrene and
377 their alkyl derivates was detected in coal in some studies, being
378 considered typical of native coals (Barrick and Prahl, 1987; Stout and

379 Emsbo-Mattingly, 2008; Achten and Hofmann, 2009). The occurrence of a
380 brown-coal deposit in Lions Cove formation (Birkenmajer et al., 1991),
381 located relatively close to the sampling sites at Penguin Island, may have
382 contributed to the PAH inputs in the region.

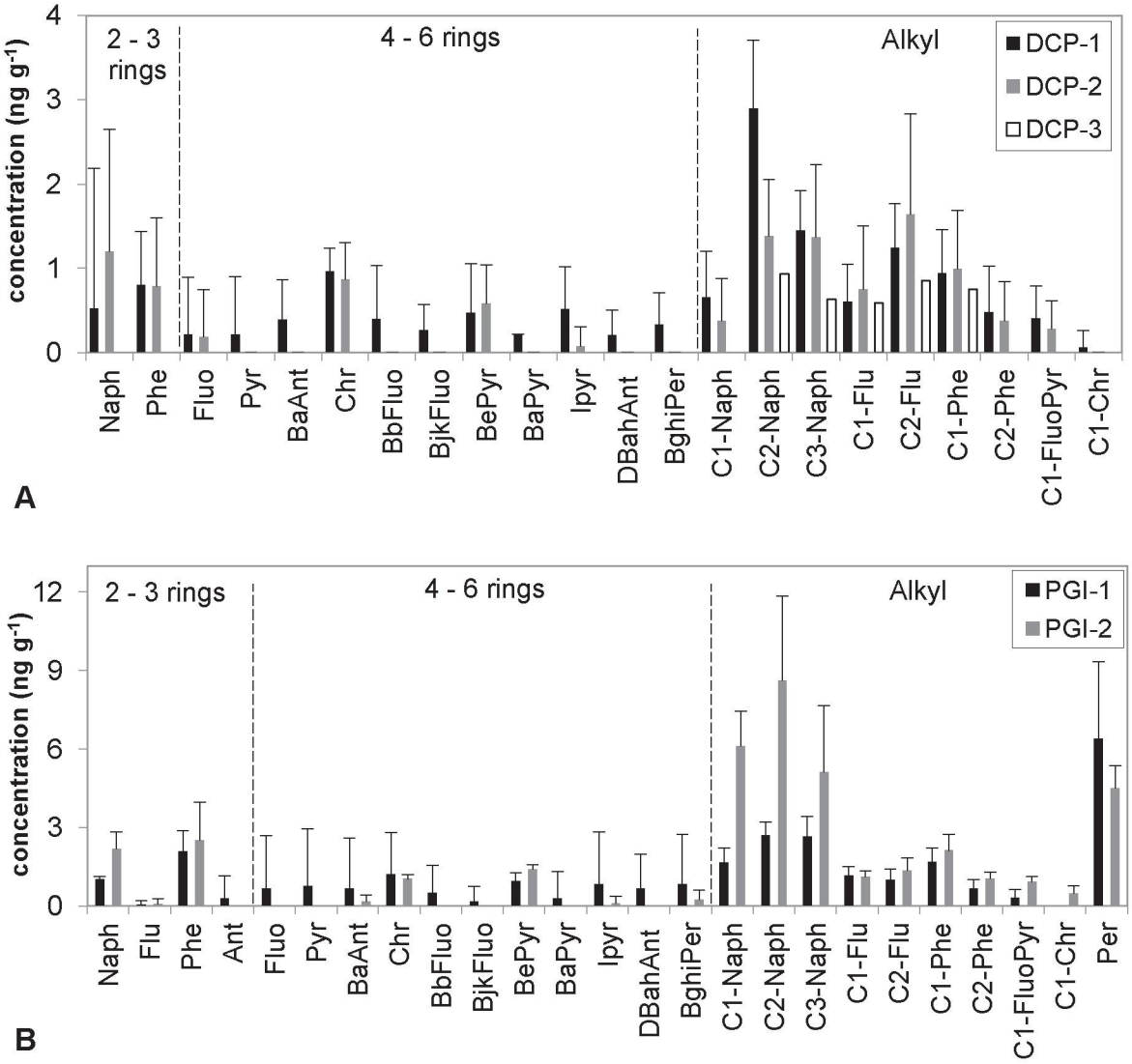

383
384
385

386 Fig. 4. Distribution of individual PAHs (mean in ng g^{-1} and standard deviation)
387 in Deception Island (A) and Penguin Island (B).
388 Naph=naphthalene; Flu=fluorene; Phe=phenanthrene; Ant=anthracene; Fluo=fluoranthene;
389 Pyr=pyrene; BaAnt= benz(*a*)anthracene; Chr=chrysene; BbFluo=benzo(*b*)fluoranthene;
390 BjkFluo= benzo(*j+k*)fluoranthene; BePyr=benzo(*e*)pyrene; BaPyr= benzo(*a*)pyrene; Ipyr=
391 indeno [1.2.3-*c,d*]pyrene; DBahAnt= dibenz(*a,h*)anthracene; BghiPer= benz(*g,h,*i)perylene;
392 C1-Naph=$\sum$-C_1-naphthanele; C2-Naph=$\sum$-C_2-naphthalene; C3-Naph=$\sum$-C_3-naphthalene; C1-
393 Flu=$\sum$-C_1-fluorene; C2-Flu=$\sum$-C_2- fluorene; C1-Phe=$\sum$-C_1-phenanthrene; C2-Phe=$\sum$-C_2-
394 phenanthrene; C1-FluoPyr=$\sum$-C_1-(fluoranthene+pyrene); C1-Chr=$\sum$-C_1-chrysene;
395 Per=Perylene.
396

397 Despite this "petrogenic" PAH pattern found in coal samples, the
398 distribution and composition may vary according to the type of coal and

399 the characteristics of the environment where it was formed. Particularly in
400 lignite (a type of brown-coal) deposits, a high concentration of perylene
401 occurs (Bojakowska and Sokołowska, 2001; Stout and Emsbo-Mattingly,
402 2008), which could have reinforced the natural inputs to the Penguin
403 Island samples, since perylene was observed in all the sections of both
404 cores, and predominantly in PGI-1.

405 Nonetheless, the distribution of PAHs in coals is similar to that
406 found in oil sources (Achten and Hofmann, 2009) and in some cases
407 analogous to that of diesel fuel arctic (DFA), a common fuel used in
408 Antarctic operations (Kennicutt et al., 1992; Taniguchi et al., 2009; Dauner
409 et al., 2015), which has high amounts of naphthalene, phenanthrene and
410 their alkyl derivates (Yu et al., 1995). Thus, a natural source of PAHs from
411 coal could mask an anthropic origin, and the data must be carefully
412 interpreted, taking into account the characteristics of each region. In our
413 data, natural inputs of PAHs derived from coal erosion in the bottom
414 sections cannot be ignored. However, anthropic sources should also be
415 considered in the top layers. The predominance of 4-6-ringed PAHs in the
416 most recent sections of PGI-1 core (1974-2007) confirms the probable
417 influence of anthropic sources over recent sections.

418 Perylene can be derived from both natural and anthropic origin
419 (Venkatesan, 1988b). The concentration of perylene over penta-aromatic
420 isomers PAHs can be used to access perylene sources, since values
421 greater than 10% probably indicate a natural origin, whereas values lower
422 than 10% are related to pyrolytic sources (Baumard et al., 1998; Readman
423 et al., 2002; Tolosa et al., 2004). Penguin Island showed all the values of
424 perylene over 5-ringed PAHs above 10% (within the range of 60-90%),
425 suggesting a natural input. An exception was seen in recent sections of
426 PGI-1 core, where the proportion decreased from 76 to 17%, indicating the
427 influence of pyrolytic sources.

428 Natural perylene has been associated with *in situ* degradation of
429 marine or terrestrial biogenic precursors (Venkatesan, 1988b; Readman et
430 al., 2002). Marine precursors include phytoplankton, mainly diatoms
431 (Venkatesan, 1988b). Formation of perylene by *in situ* degradation usually

requires anoxic environments, whereas minor levels are found at oxic sediment layers (Garrigues et al., 1988; Silliman et al., 1998). Ceschim et al. (2016) suggested that both cores were characterized by oxic sediment layers, due to the high amounts of phosphorous (P) in the samples. Thus, perylene in this case would not be formed by degradation of precursors, being deposited under oxic conditions. The weak Spearman correlation between chlorophyll-*a* (photosynthetic pigment associated with phytoplankton) and perylene in both cores (0.11 and -0.38 in PGI-1 and PGI-2, respectively) suggested that perylene was not formed by marine precursors, reinforcing a natural input derived from the erosion of coal deposits.

Another method to evaluate PAH sources is to analyse diagnostic ratios involving isomeric compounds (Martins et al., 2010; Dauner et al., 2015). According to Yunker et al. (2002), values < 0.20 for benz(*a*)anthracene to benz(*a*)anthracene + chrysene ratio (BaA/228) indicate petroleum sources, while values between 0.20 - 0.35 indicate a mixed origin (petroleum and combustion), and values > 0.35 imply a predominance of combustion sources; the indeno[1,2,3-*c,d*]pyrene to indeno[1,2,3-*c,d*]pyrene + benzo(*g,h,i*)perylene (IP/IP+Bghi) ratio indicates petroleum sources for values < 0.20, combustion from vehicle exhaustion and/or petroleum and by-products values between 0.20 to 0.50 and combustion derived from grass, wood or coal for values > 0.50.

Diagnostic ratios between unsubstituted and alkyl PAHs have also been used to access the possible PAHs sources, since alkyl PAHs are firstly associated with petroleum origin and unsubstituted PAHs (mainly 4-6 ringed) are found in combustion sources, whereas 2-3 ringed PAHs can be related to both sources (Soclo et al., 2000; Yunker et al., 2002; Zhang et al., 2008). The ratio between phenanthrene/phenanthrene + methyl-phenanthrenes (C_0-P/$\sum(C_0+C_1)$-P), indicates petroleum source for values < 0.40, while values > 0.50 suggest biomass combustion and intermediate values as 0.40 - 0.50 suggest oil combustion (Yunker et al., 2002).

When calculated, values of the BaA/228 and IP/IP+Bghi (Fig. 5) showed a predominance of oil combustion-derived PAHs for PGI-1,

465 especially in the most recent sections, where an increase in 4-6-ringed
466 PAHs was observed (Fig. S2). Values of the BaA/228 ratio in PGI-2
467 showed a mixed source from 1983 onward, probably related to mixed
468 inputs from natural and anthropic sources due to the initial development of
469 tourism around the island. In Deception Island, when calculated, both
470 ratios showed a predominance of combustion-derived PAHs along DCP-1
471 core (Fig. 5), mainly from biomass/coal combustion. In DCP-2 core these
472 ratios could not be calculated (PAH concentrations < DL).

473 The values of the C_0-P/$\sum(C_0+C_1)$-P ratio (Fig. 6) indicate
474 combustion-derived source for PAHs in all sections of PGI-1 and PGI-2
475 cores. However, phenanthrene can be derived from both pyrolytic and
476 petroleum sources, especially the latter in the absence and/or low
477 presence of 4-6-ringed PAHs (Boehm, 2006). Owing to the high presence
478 of alkyl PAHs in both cores, phenanthrene could reflect petroleum
479 sources, not combustion, as showed by the ratio.

480 An exception can be considered in recent sections of PGI-1 core
481 (1974-2007), where the amount of 4-6-ringed PAHs increase, suggesting
482 a pyrolytic source for phenanthrene. When calculated, the C_0-P/$\sum(C_0+C_1)$-
483 P ratio values showed combustion-derived sources for DCP-1 (mixed from
484 oil and biomass/coal combustion) and DCP-2 core (biomass/coal
485 combustion).

486 Although the ratios revealed combustion sources as predominant in
487 Deception Island, the composition pattern of PAHs showed a mixed
488 source for the region, due to the low levels of both alkyl and 4-6-ringed
489 PAHs in the region. The mixed source over the years in Deception Island
490 could reflect the direct input of oil from the use of several types of fuels
491 (such as DFA) and combustion-derived hydrocarbons generated by
492 scientific stations activities and vessel traffic in the area. Petrogenic
493 sources predominated mainly in the recent sections of DCP-2 (Fig. S2),
494 where the amount of alkyl PAHs was significantly higher than 4-6-ringed
495 PAHs (15.61 and 0.57, ng g^{-1}, respectively).

496 In general, the composition pattern brings evidence that the main
497 source of PAHs in Penguin Island was petrogenic. Nevertheless, this

498 “petrogenic” pattern reflects natural inputs along the cores, derived from
499 the erosion of coal deposits located in the vicinity of the island. Anthropic
500 influence appears in the recent sections of both cores, as observed by the
501 predominant combustion sources in recent sections of PGI-1 and the
502 mixed sources found in recent sections of PGI-2 (1980-2007).

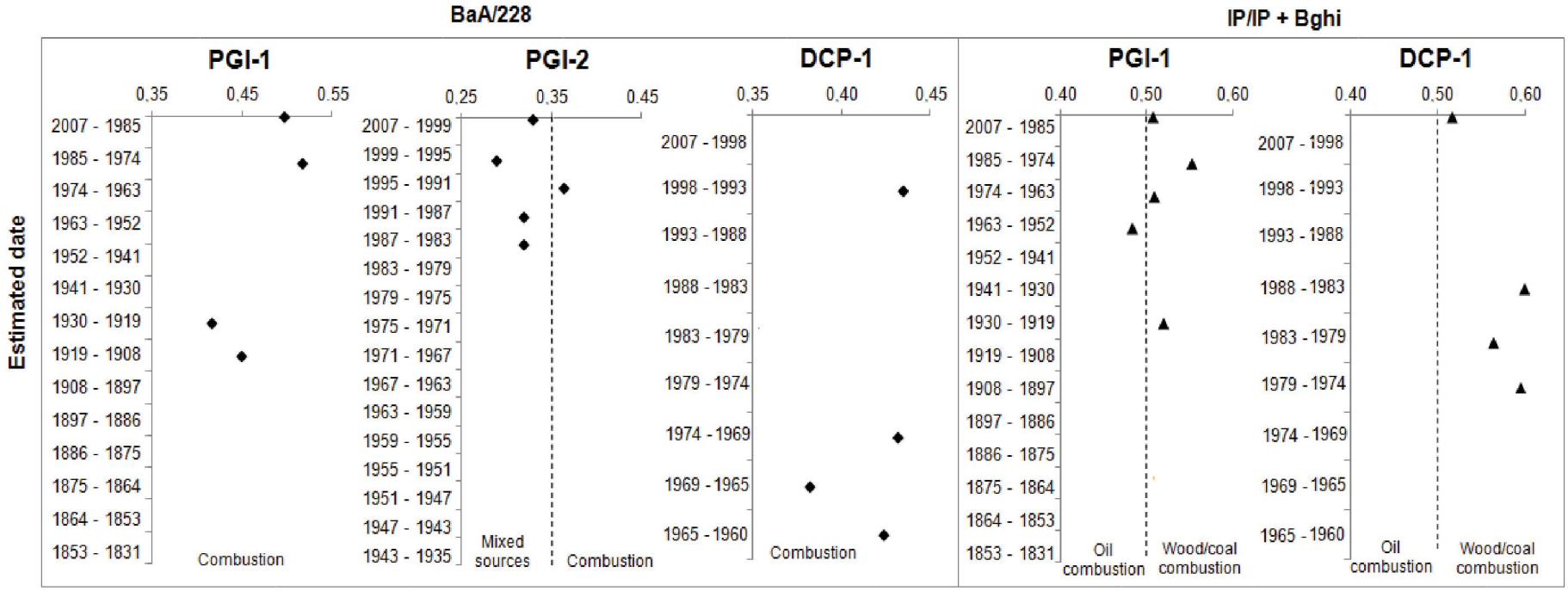

Fig. 5. PAH ratios for source identification: BaA/228 and IP/IP + Bghi (boundary lines based on values proposed by Yunker et al., 2002).

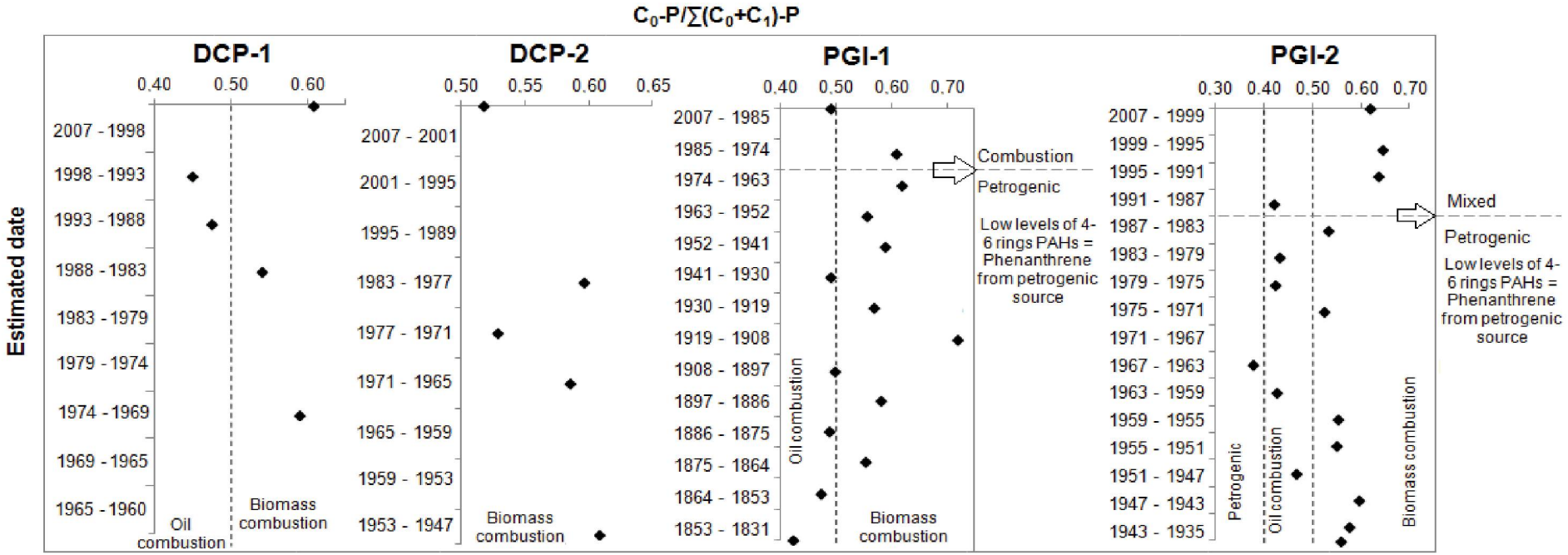

511

512 Fig. 6. PAH ratio for source identification: C_0-P/$\sum(C_0+C_1)$-P (vertical boundary lines based on values proposed by Yunker et
513 al., 2002). For PGI-1 and PGI-2 cores, a horizontal boundary with a highlighter was adopted to indicate present interpretation.

514 The mean distribution of the *n*-alkanes in Deception Island samples
515 is shown in Fig. 7A. In DCP-1, *n*-C_{22} had the highest concentrations,
516 without long (> *n*-C_{23}) or short (< *n*-C_{24}) *n*-alkane chain predominance.
517 Values of low-molecular-weight (LMW, <*n*-C_{24}) odd/even ratio showed a
518 clear predominance of even carbon chains (ratio < 0.73), whereas the
519 high-molecular-weight (HMW, >*n*-C_{23}) odd/even ratio indicated a
520 predominance of even carbon chains only in 1979-1983 and 1998-2007
521 (0.66 and 0.46, respectively). Especially in the top section (1998-2007),
522 this pattern can be related to the presence of petroleum and by-product
523 residues (Tolosa et al., 2004), given the occurrence of the entire *n*-alkane
524 sequence (*n*-C_{12} to *n*-C_{40}) and the highest value of ∑AHs and UCM found
525 in this section (19.01 μg g^{-1} and 12.18 μg g^{-1}, respectively).
526 In DCP-2, *n*-C_{17} had the highest values, also without a
527 predominance of long or short carbon chains. LMW odd/even ratios were
528 in the range of 0.90-1.06, indicating an absence of remarkable
529 predominance of odd or even carbon chains, whereas the HMW odd/even
530 ratio showed an even carbon chain predominance in 1971-1977 (0.35),
531 suggesting the presence of oil residues in this section, confirmed by the
532 occurrence of a full *n*-alkane sequence (*n*-C_{14} to *n*-C_{38}). In the remaining
533 core sections, no predominance of odd over even chains was observed
534 (values in the range of 0.83-1.21). In DCP-3, short *n*-alkane chains were
535 predominant (*n*-C_{17}, *n*-C_{16}, and *n*-C_{18}), suggesting marine sources.
536 The mean distribution of individual *n*-alkanes in Penguin Island is
537 shown in Fig. 7B. In PGI-1, *n*-C_{17} was the most abundant compound, and
538 a predominance of short *n*-alkane chain was observed, accounting for
539 70.5% of *n*-alks. The values of the LMW odd/even ratio and HMW
540 odd/even ratio were in the range of 0.96-1.66 in PGI-1, suggesting
541 discreet predominance of odd over even *n*-alkane chains. In PGI-2, *n*-C_{14}
542 was found at the highest levels, and a predominance of short chains was
543 also observed, representing 78.1% of *n*-alks. The LMW odd/even ratio
544 showed a predominance of even chains from 1947 to 1955 (values in the
545 range of 0.73-0.83), whereas the HMW odd/even ratio showed an even
546 chain predominance only in 1999-2007 (value of 0.81). In the remaining

core section, both ratios showed a slight predominance of odd over even chains (range of 0.84-1.69).

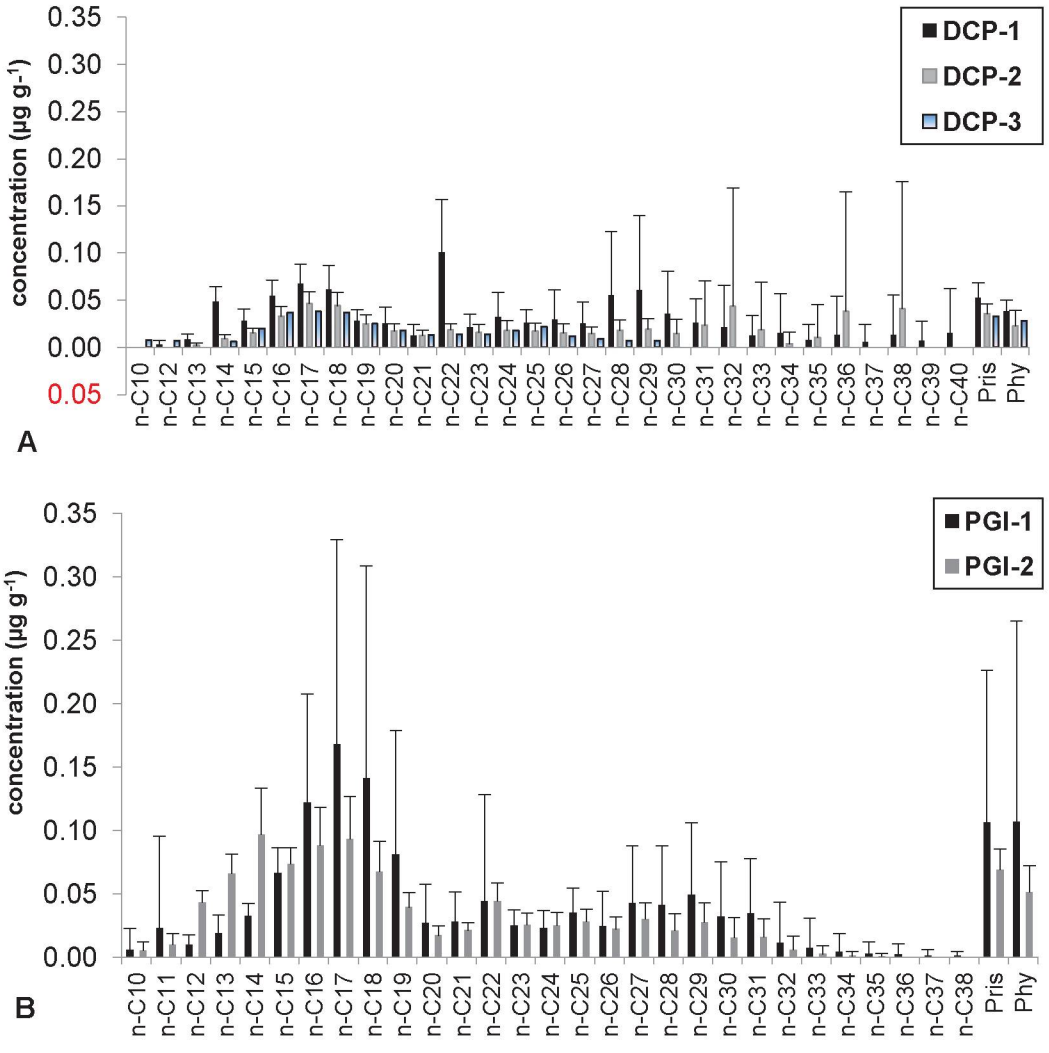

Fig. 7. Distribution of individual *n*-alkanes (mean, in µg g^{-1} and standard deviation) in Deception Island (A) and Penguin Island (B).

The distribution pattern of *n*-alkanes observed in Penguin Island could be related mainly to marine inputs derived from phytoplankton and zooplankton, considering the predominance of short *n*-alkane chains and the presence of *n*-C_{17} and *n*-C_{15} in all the samples (Harada et al., 1995). A non-predominance of odd over even chains could also be related to natural inputs, a pattern that was reported by other authors in Antarctica sediments (Venkatesan and Kaplan, 1987; Martins et al., 2004; Dauner et

563 al., 2015). According to them, *n*-alkanes in marine organisms from
564 Antarctica do not show a predominance of odd over even *n*-alkane chains
565 and can also present sequences of long chains, which can be associated
566 with oil contamination (Martins et al., 2004).

567 However, the presence of long chains in all the samples may also
568 have had an input from the coal deposit erosion, as described for PAHs,
569 since they are present in coal samples, derived from higher plants (Wang
570 and Simoneit, 1991; Stout, 1992). In this case, long *n*-alkane chains were
571 derived by multisource (marine and coal seams).

572 The carbon preference index (CPI) has been used to distinguish
573 natural from anthropogenic sources of AHs. Generally, it can be calculated
574 for long *n*-alkane chains (CPI_1) as well as short chains (CPI_2). CPI values
575 close to 1 have been related to petroleum sources and higher values to
576 contributions from higher plants (Aboul-Kassim and Simoneit, 1996;
577 Commendatore et al., 2000; Stortini et al., 2009). Due to the lack of higher
578 plants in Antarctica and the possible sequence of long *n*-alkane chains in
579 some marine organisms, the values of CPI_1 related to petroleum inputs
580 must be corroborated with other parameters (such as PAHs and UCM);
581 otherwise, the values close to 1 can indicate biogenic inputs. In fact, CPI_1
582 values close to 1 were reported in Antarctic vegetation (lichens and
583 mosses) (Cabrerizo et al., 2016), being another possible source of long *n*-
584 alkane chains. In CPI_2, values close to 1 can be related mainly to biogenic
585 inputs, due the different distribution of *n*-alkanes in Antarctica (as
586 described previously). However, values much lower than 1 can indicate
587 petroleum inputs if corroborated with other parameters. In addition, the
588 UCM/Σ*n*-alkanes (UCM/*n*-alks) ratio may be used as an indicator of
589 petroleum input: values >10 suggest the presence of degraded petroleum,
590 whereas lower values can indicate fresh oil or natural inputs (in the
591 absence of a possible anthropogenic source) (Simoneit, 1982; Tolosa et
592 al., 2004). The Fig. 8 shows a comparative plot between CPI_1 and UCM/*n*-
593 alks indexes.

594 CPI_1 values (calculated as = $0.5*(((\sum C_{25}\text{-}C_{33}) / (\sum C_{24}\text{-}C_{32})) + ((\sum C_{25}\text{-}C_{33})/(\sum C_{26}\text{-}C_{34})))$ showed a clear predominance of natural contributions in
595

596 Penguin Island (values in the range of 0.90 - 2.26), confirmed by values of
597 UCM/*n*-alks (mean of 5.78 ± 2.29 for PGI-1 and 4.39 ± 2.23 for PGI-2).
598 Only at the top section of PGI-2, CPI_1 and UCM/*n*-alks values indicate
599 petrogenic sources. CPI_1 levels showed a petrogenic contribution in the
600 top section of DCP-1, while the lower value of UCM/*n*-alks (4.92) in this
601 same section indicates recent oil input, confirming petroleum sources.
602 Relative high values of UCM/*n*-alks from 1960 - 1988 in DCP-1
603 (9.15 - 18.60) suggest the presence of degraded petroleum in these
604 sections. However, it was not indicated by CPI_1 values, reflecting a
605 possible mixed source (biogenic and petrogenic). Despite CPI_1 and
606 UCM/*n*-alks values suggests petrogenic source for 1979-1983, it could be
607 related to mixed sources, due to the absence of a significant increase of
608 parameters as AHs, UCM and PAHs.
609 In DCP-2 core, values of CPI_1 showed petrogenic inputs in 1971 -
610 1977. In the same section, low value of the UCM/*n*-alks ratio was found
611 (2.41), reflecting the presence of preserved oil derivates in the sediment,
612 confirmed by a slight increase in PAHs. The highest values of UCM/*n*-alks
613 ratio were observed in 1947 - 1965 (values in the range of 10.5 - 17.0),
614 followed by 1977 - 1989 (values in the range of 11.9 - 12.4) and at the top
615 of the core (11.8), indicating petroleum sources. However, it was not
616 indicated by CPI_1 values, suggesting mixed sources in these sections of
617 DCP-2. CPI_1 and UCM/*n*-alks values for DCP-3 (1.51 and 9.83,
618 respectively) suggest natural inputs, confirmed by the *n*-alkanes
619 distribution pattern.
620

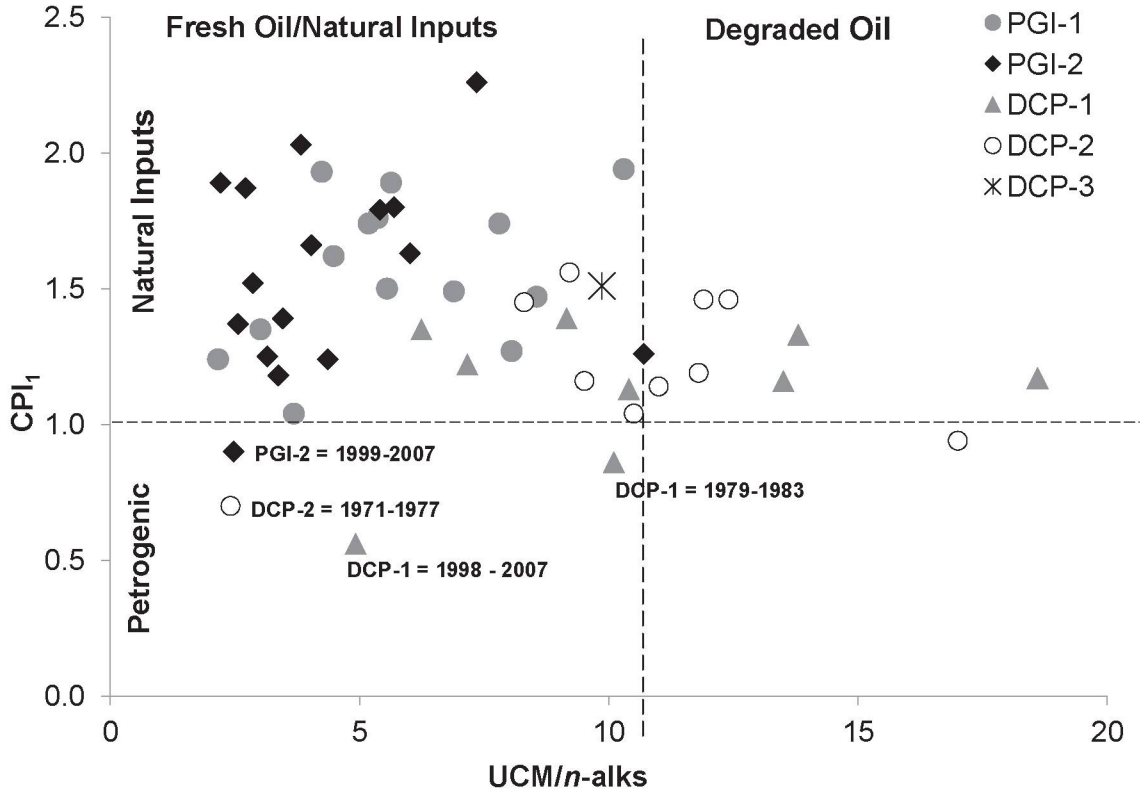

621

622 Fig. 8. Plot between CPI_1 (long *n*-alkanes chains) and UCM/*n*-alks ratios for
623 PGI-1, PGI-2, DCP-1 and DCP-2 cores and DCP-3 (surficial sediment).

624 CPI_2 (calculated as = $0.5^* (((\sum C_{13}\text{-}C_{21}) / (\sum C_{12}\text{-}C_{20})) + ((\sum C_{13}\text{-}$
625 $C_{21})/(\sum C_{14}\text{-}C_{22}))))$ ranged from 1.01 to 1.35 in PGI-1 and from 0.78 to 1.72
626 in PGI-2. The values found in Penguin Island can be related to natural
627 inputs, as reported in CPI_1, confirming the predominance of biogenic
628 source for *n*-alkanes in the region. In DCP-1, values were found in the
629 range of 0.54 to 0.71 and in DCP-2 from 0.82 to 1.00. Only in the top
630 section of DCP-1 the value of CPI_2 (0.57) can be related to petroleum
631 inputs, as observed in CPI_1 and UCM/*n*-alks ratios. In DCP-2, the value of
632 CPI_2 (0.82) from 1971 - 1977 was related to petroleum inputs, in
633 agreement with the CPI_1 and UCM/*n*-alks ratios. In the remaining of the
634 cores sections the values of CPI_2 were probably reflecting mixed sources,
635 as reported in CPI_1 and UCM/*n*-alks ratios. In DCP-3 CPI_2 was also
636 indicating biogenic value (0.89), in agreement with the other ratios.

637 The isoprenoid hydrocarbons pristane and phytane were present in
638 all samples. They are found in petroleum by-products, and their natural
639 source usually is associated with degradation of phytyl side chains present

640 in chlorophyll-*a* (Volkman et al., 1992; Bícego et al., 2009). However,
641 pristane has also been associated with direct input from zooplankton
642 (Volkman et al., 1992), and both have been related to archaeal lipids
643 (Rowland, 1990).

644 The values of pristane and phytane occurred in similar levels along
645 the cores in Penguin Island, except for the recent sections of PGI-2 core,
646 where pristane predominated. This pattern was similar to data previously
647 observed in waters and in biota collected in Bransfield Strait (Cripps,
648 1989), suggesting that ratios involving isoprenoids in this case would not
649 be indicative of environmental pollution. A strong Spearman correlation
650 between pristane and phytane with short *n*-alkane chains (0.87 and 0.90
651 for PGI-1; 0.83 and 0.85 for PGI-2, respectively) suggests the same
652 source for these compounds, probably derived from marine inputs. The
653 absence of a correlation with chlorophyll-*a* may reflect multiple sources for
654 these compounds, in agreement with observations made by Ceschim et al.
655 (2016), which suggests multiple sources of sedimentary organic matter in
656 Penguin Island, due to the distinct contributions of sterols related to
657 zooplankton, macroalgae, and microalgae.

658 In DCP-1, the values of pristane and phytane were also similar
659 along the core. A strong correlation with ∑AHs and UCM in this case
660 (pristane = 0.75 and 0.74 and phytane 0.69 and 0.79, respectively) can
661 indicate petrogenic sources for these compounds. In DCP-2, the
662 predominance of pristane in almost the entire core (from 1959-2001) could
663 be related to phytoplankton inputs (Readman et al., 2002). Although site
664 DCP-3 showed similar levels of pristane and phytane, a marine source
665 may be assumed, as observed by CPI_1 and CPI_2 values.

666 Tricyclic terpane series ranging from C_{20} to C_{26} were detected in
667 Deception Island, with a predominance of the C_{23}-tricyclic terpane. DCP-2
668 also showed the presence of the C_{24}- tetracyclic terpane. Hopane series
669 ranging from C_{27} to C_{30} with the predominance of the 17α,21β
670 configuration were detected in 1965-1969 at DCP-1 and in all sections of
671 the DCP-2 core. On average, C_{30}-17α,21β-Hopane was predominant in
672 the samples. The highest values of terpanes and hopanes in DCP-2 were

673 detected in 1965-1971 (35.45 and 22.10 ng g^{-1}, respectively), where a pair
674 of C_{31}-diastereoisomers (22R, 22S) was also observed, with a value of
675 0.48 for the ratio C_{31}-αβ 22S/C_{31}-αβ 22S + C_{31}-αβ 22R, which is very close
676 to the equilibrium value of 0.60 found in typical petroleum (Aboul-Kassim
677 and Simoneit, 1996), reinforcing a petrogenic input in this section.
678 The composition and distribution patterns of petroleum biomarkers
679 observed in Deception Island suggest a petrogenic input (Silva and
680 Bícego, 2010), probably related to the use of fossil fuels to power
681 generation and for the different types of vessels that operate in Antarctic
682 waters. Petroleum products used in the Antarctic include DFA, special
683 Antarctic blend diesel (SAB), lubricating and engine oils, petrol, marine
684 gas oil and other marine diesels, representing a source of these
685 biomarkers to the environment (Green and Nichols, 1995; Snape et al.,
686 2005; Wang et al., 2006; Raymond et al., 2016), even in lower amounts as
687 those observed in Deception Island.
688 A tricyclic terpane series ranging from C_{20} to C_{25} were detected in
689 sediments from Penguin Island. These compounds could be related
690 mainly to the erosion of coal deposits, as they had been recorded in coal
691 samples (Simoneit et al., 1986; Liu et al., 1991). Tricyclic terpanes in coal
692 are derived from algal and bacterial precursors, from terrestrial plant
693 debris (especially the C_{20}-tricyclic terpane), and from the thermal
694 degradation of pentacyclic triterpanes (as hopanes) (Liu et al., 1991;
695 Schwarzbauer and Jovančićević, 2015). Unexpectedly, no correlation
696 between PAHs and terpanes was detected, probably due to the
697 multisource nature of PAHs in the region (natural from erosion of coal
698 deposits and the burning of fossil fuel, particularly in the recent sections).
699
700 *2.4.3 PCA*
701
702 A PCA model was adopted to evaluate the main hydrocarbon
703 sources in each core (Fig. 9), as well as to determine if the sediment grain
704 size distribution (silt+clay) and chlorophyll-*a* values (in Penguin Island)

were factors that may have influenced the hydrocarbon accumulation in sediments

In DCP-1, the principal component (PC) 1 explained 62.4% of the data variability, being positively correlated with PAHs (2-3 ringed, 4-6 ringed and alkyl), grain size, AHs, UCM, *n*-alkanes and negatively correlated with terpanes. The grain size distribution in DCP-1 was related mainly with alkyl, 4-6 ringed PAHs and short *n*-alkanes chain, suggesting that the accumulation of these compounds are related to the deposition of the fine fraction sediments. PCA revealed that from 1988 to 1998 the sources in the region were mixed (grouped near combustion and petrogenic related PAHs), whereas from 1998 to 2007 a petrogenic source was predominant, as reported in CPI_1, CPI_2 and UCM/*n*-alks values. PC2 explained 15.4% of the data and was related mainly to hopanes. PCA confirmed the presence of degraded petroleum by-products in sediments from 1960-1969, as reported by the UCM/*n*-alks values.

In DCP-2, PC1 explained 33.9% of the data and was negatively correlated with hopanes, terpanes, *n*-alkanes and 4-6 ringed PAHs. PC2 explained 28.8% of the data, being positively correlated with alkyl, UCM, AHs and 2-3 ringed PAHs (petrogenic-related PAHs). PCA revealed that samples from the bottom core sections (A = 1947 to 1965) had little anthropogenic influence, whereas samples from the middle sections until the top of the core (B = 1965 to 2007) were grouped near petroleum-related hydrocarbons. This is in agreement with the hydrocarbons distribution, which showed an increase in petrogenic sources in the top sections. From 1971 - 1977, a petroleum input is suggested due presence of PBMs, as well as by the CPI_1, CPI_2 and UCM/*n*-alks ratios values.

In PGI-1, PC1 explained 28.6% of the data variability and was related mainly with the grain size distribution (positively correlated); and 2-3 ringed PAHs, AHs, UCM, and long *n*-alkanes chains (negatively correlated). PC2 represents 23.2% of the data, being related mainly to chlorophyll-*a* (positively correlated), whereas 4-6 ringed PAHs were probably explained by another principal component. PC2 was negatively correlated with alkyl, short *n*-alkane chains and terpanes. PCA

738 discriminate among samples from the bottom and middle core sections (A
739 = 1831 to 1952), being positively correlated with the grain size and with
740 compounds related to natural sources (short chains, chlorophyll-*a* and
741 those related to erosion of coal deposits = alkyl PAHs and terpanes). From
742 1952 until the top sections (B) a change in hydrocarbons sources was
743 observed, being correlated mainly with anthropogenic-related compounds
744 (UCM, AHs and 2-3 ringed PAHs), especially in the top section. The grain
745 size in this core was influencing mainly the deposition of alkyl, terpanes
746 and short *n*-alkanes chain.

747 In PGI-2, PC1 represents 27.8% of the data and was related to 2-3
748 and 4-6-ringed PAHs (positively correlated), long *n*-alkanes chains, AHs
749 and UCM (negatively correlated). PC2 explained 23.0% of the data,
750 related mainly to chlorophyll-*a* (negatively correlated), short *n*-alkane
751 chains, terpanes, grain size and alkyl (positively correlated). PCA also
752 made discrimination from the top sections of the core (A=1995 to 2007),
753 with samples grouped near anthropogenic compounds (2-3 and 4-6-ringed
754 PAHs), whereas the ancient sections (1935 - 1955) were grouped near
755 natural-related inputs (chlorophyll-*a*). Grain size also influenced mainly the
756 deposition of alkyl and terpanes, as observed in PGI-1 core.
757

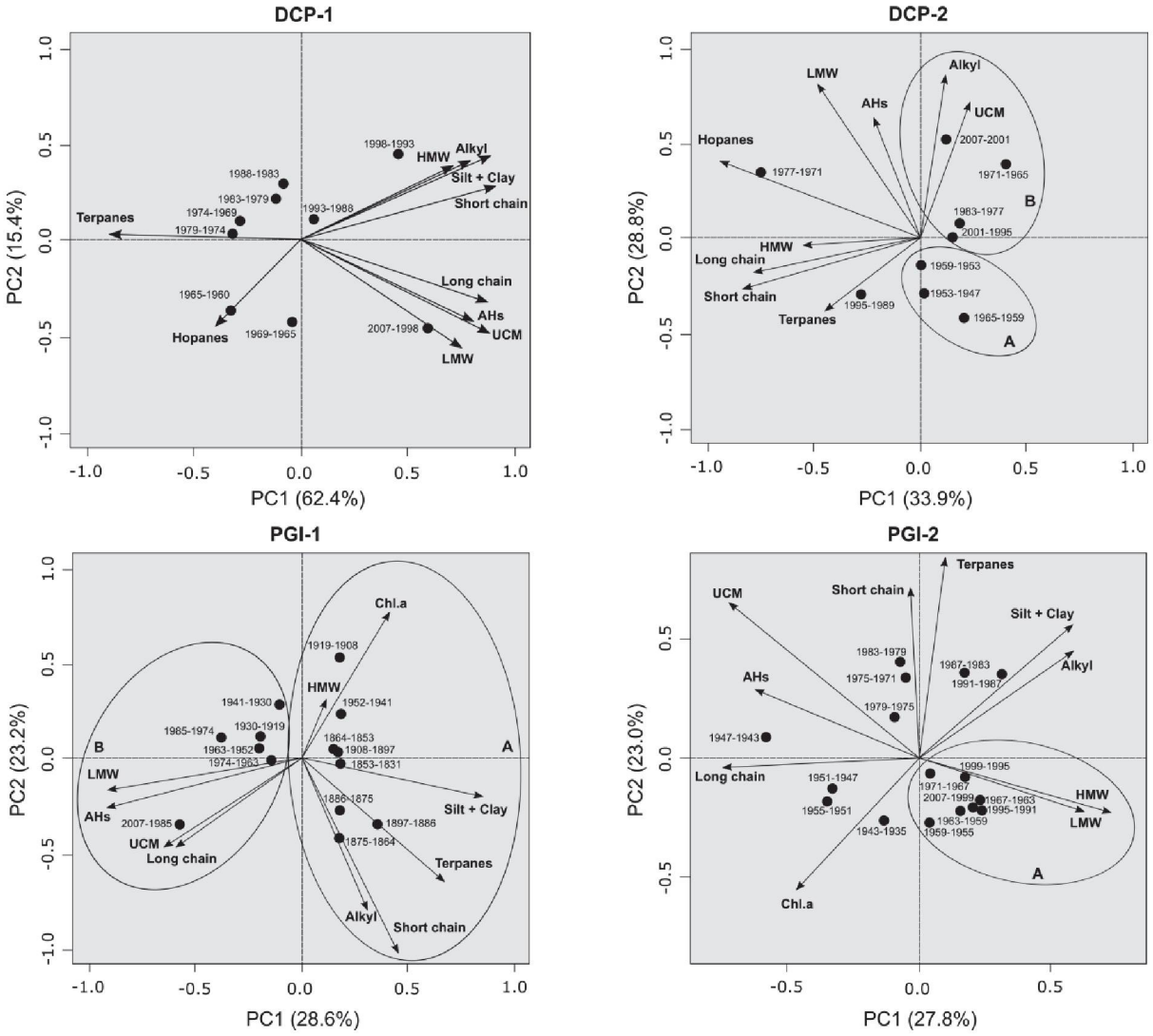

Fig. 9. Plot of the principal component analysis (PCA) loadings and scores for DCP-1, DCP-2, PGI-1 and PGI-2 cores.

*Silt+Clay: Sum of percentage of silt and clay in the samples. HWM= 4-6 ring PAHs. LMW= 2-3 ring PAHs. Short chain: $\sum<n\text{-}C_{24}$. Long chain: $\sum>n\text{-}C_{23}$. *DCP-1: without grain size (no data available).

762 *2.4.4 Historical record of hydrocarbons in Deception and Penguin islands*
763
764 The maximum level of ∑PAHs in DCP-1 core was detected in 1993-
765 1998, followed by 1998-2007. Slight increases in ΣAHs, *n*-alks and UCM
766 levels from the bottom until the recent sections were observed, reaching
767 maximum concentrations in the top layer (1998-2007). In DCP-2 core, the
768 highest levels of ∑PAHs were reported in 2001-2007 and in 1971-1977,
769 whereas the highest levels of ∑AHs were found in 1971-1977 and in 1989-
770 1995.
771 Unexpectedly, a significant increase in the levels of PAHs during
772 the years of volcanic eruptions (1967, 1969 and 1970) did not occur. This
773 could be explained by the fact that volcanic eruptions do not necessarily
774 act as a direct source in PAH formation but as a transport/scavenger
775 mechanism. The combustion of the available organic material during
776 eruptions, such as vegetation (as lichens and mosses), could release
777 PAHs (Pereira et al., 1980; Stracquadanio et al., 2003). However, the
778 vegetation is scarce in this region, and the PAHs in the sediments from
779 Deception Island are probably not from these events. Instead, the slight
780 increase in PAHs reported in DCP-2 from 1965-1977 could be associated
781 mainly with the development and increase in scientific activities around
782 Fumarole Bay, as also evidenced by the increase of petroleum
783 biomarkers, ΣAHs, *n*-alks and UCM values in this same period.
784 The levels of ΣPAHs, ΣAHs and PBMs found from 1990 onward in
785 both cores from Deception Island could be a result of the development of
786 tourism in the region, as well as the establishment of a Spanish scientific
787 station (Smith Jr. et al., 2003), which increased the use of fossil fuels.
788 Despite some events found in Deception Island, a clear tendency of
789 hydrocarbons was not observed, since the levels did not vary significantly
790 throughout the cores.
791 The highest values of ∑PAHs in Penguin Island cores were
792 reported in recent sections, from 1974-2007 in PGI-1 (values reaching
793 55.99 ng g^{-1}) and from 1987-2007 in PGI-2 (values reaching 60.34 ng g^{-1}).
794 PGI-1 showed a slight increase in ∑AHs from 1908 until the recent layers,

795 with the highest level in 1974-1985. PGI-2 showed higher values of ΣAHs
796 and UCM in 1943-1947, and it showed a slight increase in the recent
797 sections. In the deeper sections of the cores, the presence of PAHs and
798 AHs could be related mainly to natural inputs, given the low levels of UCM;
799 the absence of biomarkers related to petroleum (as hopanes); the
800 presence of terpanes related to the erosion of coal deposits; and the
801 marine biogenic *n*-alkane origin observed in the compound distribution. An
802 anthropogenic origin of hydrocarbons for the deeper sections is
803 inconsistent with the history of anthropic activities of the region, and the
804 PAH levels are probably derived from natural inputs by the erosion of coal
805 deposits, acting as a continuous contributor, as discussed above.
806 However, an input from both natural and anthropogenic sources of
807 PAHs and AHs in the recent sections needs to be considered for both
808 cores, especially after 1970. The anthropogenic source was reported by
809 the increase in combustion-related compounds in recent sections of PGI-
810 1, reflecting a possible deposition from atmospheric inputs, and by CPI_1
811 values in the top section of PGI-2, showing a petrogenic source. The
812 period from 1950-1990 was marked by the building of several scientific
813 stations around King George Island, increasing the use of fuel for snow
814 vehicles, power generation and local boating, as well as the initial
815 development of tourism (Bícego et al., 2009; Martins et al., 2010), which
816 could have contributed to the atmospheric input of PAHs.
817

818 **2.5 Conclusions**

819

820 The determination of hydrocarbons in the sediment cores of
821 Deception and Penguin Island allowed an assessment of the main sources
822 of these compounds in the region and established a relationship with the
823 characteristics of each area. Relatively low levels of hydrocarbons were
824 reported in our study, and the results were compared to those found in
825 other pristine regions of Antarctica.
826 Deception Island showed a similar pattern distribution in both cores,
827 with mixed sources for the analysed hydrocarbons, including combustion,

828 petrogenic, and natural contributions. An increasing tendency in
829 petrogenic PAH inputs was found in the recent sections, as observed in
830 the CPI_1, CPI_2 and UCM/*n*-alk ratios in DCP-1 and by the PCA in DCP-2.
831 No predominance of long or short *n*-alkane chain was found in the cores,
832 and little dominance of odd over even carbon chains was detected. This
833 pattern was related to a probable mixed source (natural and anthropic) of
834 *n*-alkanes in the majority of the core sections. In the surficial sediment
835 (DCP-3), *n*-alkanes related to marine inputs were reported, with short
836 carbon chain dominance. The presence of anthropogenic hydrocarbons in
837 Deception was related mainly to tourism and scientific station activities,
838 such as the use of fossil fuels for energy and vessel traffic.

839 Penguin Island showed relatively high values of alkyl PAHs, with a
840 "petrogenic" pattern. However, it was associated mainly with natural
841 inputs, which were derived from coal deposits that are located in the
842 vicinity of the island, a factor that needs to be considered in future studies
843 in the region. Short *n*-alkane chains were predominant in the region,
844 reflecting strong marine inputs, as also evidenced by CPI_1 and CPI_2 values
845 and by the isoprenoids hydrocarbons. Marine sources for the region were
846 derived from distinct contributions (zooplankton, macro and microalgae).
847 Terpanes found in the region were also associated with coal contributions.
848 In the recent sections of both cores, anthropogenic hydrocarbons were
849 reported due to the increase of combustion-derived compounds in PGI-1
850 and by the values observed by CPI_1 and UCM/*n*-alks for PGI-2. The
851 anthropogenic-related hydrocarbons in the recent sections were
852 associated with tourism activities, the increase in vessel traffic and the
853 atmospheric deposition of PAHs.

854 Despite being located in remote areas (especially Penguin Island),
855 both islands showed evidence of anthropogenic-derived contaminants,
856 with a growing tendency in recent years. This constant increase can lead
857 to a chronic pollution and, as a consequence, to negative effects to the
858 biota and severe degradation of Antarctic ecosystems. The scientific
859 stations located in Deception Island could use renewable sources of
860 energy and effective law enforcement for the ships operating in both

areas, as heavy-grade fuel oil has been already prohibited in Antarctica. Additionally, continuous and long-term monitoring of hydrocarbons is highly advised, as these compounds are an important tool in the assessment of human impacts. This monitoring would facilitate the tracking of principal sources of the contaminants and their trends, and this tracking could lead to the determination of priority sites for environmental monitoring. Such scientific work would certainly be helpful in the improvement of environmental policies and management plans, favouring a potential reduction of human traces and risks to the Antarctic fauna and flora.

2.6 Acknowledgements

The work was supported by the Antarctic Brazilian Program (PROANTAR), Secretaria da Comissão Interministerial para os Recursos do Mar (SECIRM), Ministério de Ciência, Tecnologia e Inovação (MCTI) and National Council for Scientific and Technological Development (CNPq, 550014/2007-1 and 442692/2018-8). M. Sutilli would like to thank CAPES (Coordenação de Aperfeiçoamento de Pessoal de Ensino Superior) for the M.Sc. Scholarship. The authors wish to thank the NApOc Ary Rongel staff and Dr. J. A. Ferreira for support during the sampling activities and preliminary sample. The authors also thank MSc. A. L. L. Dauner for the map and MSc. M. R. Garcia for assistance in petroleum biomarkers analyses. This study was developed as part of the Graduate program in estuarine and ocean systems at the Federal University of Paraná (PGSISCO-UFPR).

2.7 References

Aboul-Kassim, T. a T., Simoneit, B.R.T., 1996. Lipid geochemistry of surficial sediments from the coastal environment of Egypt I. Aliphatic hydrocarbons-characterization and sources. **Marine Chemistry** 54, 135–158. doi:10.1016/0304-4203(95)00098-4

895 Achten, C., Hofmann, T., 2009. Native polycyclic aromatic hydrocarbons
896 (PAH) in coals - A hardly recognized source of environmental
897 contamination. **Science of the Total Environmen**t 407, 2461–2473.
898 doi:10.1016/j.scitotenv.2008.12.008
899
900 Aronson, R.B., Thatje, S., Mcclintock, J.B., Hughes, K.A., 2011.
901 Anthropogenic impacts on marine ecosystems in Antarctica. **Annals of**
902 **the New York Academy of Sciences** 1223, 82–107. doi:10.1111/j.1749-
903 6632.2010.05926
904
905 Baker, P.E., McReath, M.A., Harvey, M.R., Roobol, M.J., Davies, T.G.,
906 1975. The geology of the South Shetland Islands: V - volcanic evolution of
907 Deception Island. **British Antarctic Survey Scientific Reports** 78.
908
909 Bargagli, R., 2008. Environmental contamination in Antarctic ecosystems.
910 **Science of the Total Environment**, 400, 212–226.
911 doi:10.1016/j.scitotenv.2008.06.062
912
913 Barrick, R.C., Prahl, F.G., 1987. Hydrocarbon Geochemistry of the Puget
914 Sound Region-III. Polycyclic Aromatic Hydrocarbons in Sediments.
915 **Estuarine, Coastal and Shelf Science** 25, 175–191.
916
917 Baumard, P., Budzinski, H., Michon, Q., Garrigues, P., Burgeot, T.,
918 Bellocq, J., 1998. Origin and bioavailability of PAHs in the Mediterranean
919 Sea from Mussel and Sediment Records. **Estuarine, Coastal and Shelf**
920 **Science** 47, 77–90. doi:10.1006/ecss.1998.0337
921
922 Bengston, S., 2011. Persistent organic pollutants in Antarctica: current and
923 future research priorities. **Journal of Environmental Monitorin**g 13, 497–
924 504. doi:10.1039/c0em00230e
925
926 Bícego, M.C., Zanardi-Lamardo, E., Taniguchi, S., Martins, C.C., da Silva,
927 D.A.M., Sasaki, S.T., Albergaria-Barbosa, A.C.R., Paolo, F.S., Weber,
928 R.R., Montone, R.C., 2009. Results from a 15-year study on hydrocarbon
929 concentrations in water and sediment from Admiralty Bay, King George
930 Island, Antarctica. **Antarctic Science** 21, 209.
931 doi:10.1017/S0954102009001734
932
933 Birkenmajer, K., Frankiewicz, J.K., Wagner, M., 1991. Tertiary coal from
934 the Lions Cove Formation, King George Island, West Antarctica. **Polish**
935 **Polar Research** 229–241.
936

937 Boehm, P. D., 2006. **Polycyclic Aromatic Hydrocarbons (PAHs)**. In:
938 MORRISON, R.; MURPHY, B. Environmental Forensics: A contaminant
939 specific approach. Elsevier, San Diego, p. 533
940
941 Bojakowska, I., Sokołowska, G., 2001. Polycyclic aromatic hydrocarbons
942 in hard coals from Poland. **Geological Quarterly** 45, 93–98.
943
944 Bouloubassi, I., Saliot, a., 1993. Investigation of anthropogenic and natural
945 organic inputs in estuarine sediments using hydrocarbon markers (NAH,
946 LAB, PAH). **Oceanologica Acta** 16, 145–161.
947
948 Braun, M., Saurer, H., Vogt, S., Simo, J.C., 2001. The Influence of Large-
949 Scale Atmospheric Circulation on The Surface Energy Balance of The
950 King George Island Ice Cap. **International Journal of Climatology** 36,
951 21–36. doi:10.1002/joc.563/pdf
952
953 Cabrerizo, A., Tejedo, P., Dachs, J., Benayas, J., 2016. Anthropogenic
954 and biogenic hydrocarbons in soils and vegetation from the South
955 Shetland Islands (Antarctica). **Science of the Total Environment** 569–
956 570, 1500–1509. doi:10.1016/j.scitotenv.2016.06.240
957 Ceschim, L.M.M., Dauner, A.L.L., Montone, R.C., Figueira, R.C.L.,
958 Martins, C.C., 2016. Depositional history of sedimentary sterols around
959 Penguin Island, Antarctica. **Antarctic Science** 12, 1–12.
960 doi:10.1017/S0954102016000274
961
962 Cincinelli, A., Martellini, T., Bittoni, L., Russo, A., Gambaro, A., Lepri, L.,
963 2008. Natural and anthropogenic hydrocarbons in the water column of the
964 Ross Sea (Antarctica). **Journal of Marine Systems** 73, 208–220.
965 doi:10.1016/j.jmarsys.2007.10.010
966
967 Combi, T., Taniguchi, S., Figueira, R.C.L., Mahiques, M.M. De, Martins,
968 C.C., 2013. Spatial distribution and historical input of polychlorinated
969 biphenyls (PCBs) and organochlorine pesticides (OCPs) in sediments from
970 a subtropical estuary (Guaratuba Bay, SW Atlantic). **Marine Pollution**
971 **Bulletin** 70, 247–252. doi:10.1016/j.marpolbul.2013.02.022
972
973 Commendatore, M.G., Esteves, J.L., Colombo, J.C., 2000. Hydrocarbons
974 in coastal sediments of Patagonia, Argentina: Levels and probable
975 sources. **Marine Pollution Bulletin** 40, 989–998. doi:10.1016/S0025-
976 326X(00)00042-4
977

978 Cripps, G.C., 1989. Problems in the identification of anthropogenic
979 hydrocarbons against natural background levels in the Antarctic. **Antarctic**
980 **Science** 1, 307–312. doi:10.1017/S0954102089000465
981
982 Curtosi, A., Pelletier, E., Vodopivez, C.L., Mac Cormack, W.P., 2007.
983 Polycyclic aromatic hydrocarbons in soil and surface marine sediment
984 near Jubany Station (Antarctica). Role of permafrost as a low-permeability
985 barrier. **Science of the Total Environment** 383, 193–204.
986 doi:10.1016/j.scitotenv.2007.04.025
987
988 Dauner, A.L.L., Hernández, E.A., MacCormack, W.P., Martins, C.C., 2015.
989 Molecular characterisation of anthropogenic sources of sedimentary
990 organic matter from Potter Cove, King George Island, Antarctica**. Science**
991 **of the Total Environment** 502, 408–416.
992 doi:10.1016/j.scitotenv.2014.09.043
993
994 Dibbern, J.S., 2010. Fur seals, whales and tourists: a commercial history
995 of Deception Island, Antarctica. **Polar Record** 46, 210–221.
996 doi:10.1017/S0032247409008651
997
998 Ferron, F.A., Simoes, J.C., Aquino, F.E., Setzer, A.W., 2004. Air
999 Temperature Time Series for King George Island, Antarctica. **Brazilian**
1000 **Antarctic Research** 4, 155–169.
1001
1002 Flexas, M.A.R.M., Arias, M.R., Ojeda, M.A., 2017. Hydrography and
1003 dynamics of Port Foster, Deception Island, Antarctica. **Antarctic Science**
1004 29, 83–93. doi:10.1017/S0954102016000444
1005
1006 Garrigues, P., Parlanti, E., Lapouyade, R., Bellocq, J., 1988. Distribution of
1007 methylperylene isomers in selected sediments. **Geochimica et**
1008 **Cosmochimica Acta** 52, 901–907.
1009
1010 Green, G., Nichols, P.D., 1995. Hydrocarbons and Sterols in Marine
1011 Sediments and Soils at Davis Station, Antarctica: A Survey for Human-
1012 Derived Contaminants. Antarctic Science 7, 137–144.
1013 doi:10.1017/S0954102095000198
1014
1015 Guerra, R., Fetter, E., Cheschim, L.M.M., Martins, C.C., 2011. Trace
1016 metals in sediment cores from Deception and Penguin Islands (South
1017 Shetland Islands, Antarctica). **Marine Pollution Bulletin** 62, 2571–2575.
1018 doi:10.1016/j.marpolbul.2011.08.012
1019

1020 Harada, N., Handa, N., Fukuchi, M., Ishiwatari, R., 1995. Source of
1021 hydrocarbons in marine sediments in Lutzow-Holm Bay, Antarctica.
1022 **Organic Geochemistry** 23, 229–237.
1023
1024 IAEA, International Atomic Energy Agency, Reference sheet for RM IAEA-
1025 408. IAEA, Vienna, 8pp.
1026
1027 Kennicutt II, M.C., McDonald, T.J., Denoux, G.J., McDonald, S.J., 1992.
1028 Hydrocarbon Contamination on the Antarctic Peninsula. I. Arthur Harbor -
1029 Subtidal sediments. **Marine Pollution Bulletin** 24, 499–506.
1030
1031 Kim, M., Kennicutt, M.C., Qian, Y., 2006. Molecular and stable carbon
1032 isotopic characterization of PAH contaminants at McMurdo Station,
1033 Antarctica. **Marine Pollution Bulletin** 52, 1585–1590.
1034 doi:10.1016/j.marpolbul.2006.03.024
1035
1036 Lenihan, H.S., Oliver, J.S., Oakden, J.M., Stephenson, M.D., 1990.
1037 Intense and localized benthic marine pollution around McMurdo Station,
1038 Antarctica. **Marine Pollution Bulletin** 21, 422–430. doi:10.1016/0025-
1039 326X(90)90761-V
1040
1041 Liu, Y., Zhang, P., Wu, Q., 1991. The biomarker hydrocarbons and the
1042 organic geochemical characteristics of fu-shun bituminous coal. **Fuel**
1043 **Science and Technology International** 9, 745–767.
1044 doi:10.1080/08843759108942293
1045
1046
1047 Martins, C.C., Bícego, M.C., Taniguchi, S., Montone, R.C., 2004. Aliphatic
1048 and polycyclic aromatic hydrocarbons in surface sediments in Admiralty
1049 Bay, King George Island, Antarctica. **Antarctic Science** 16, 117–122.
1050 doi:10.1017/S0954102004001932
1051
1052 Martins, C.C., Bícego, M.C., Rose, N.L., Taniguchi, S., Lourenzo, R. a.,
1053 Figueira, R.C.L., Mahiques, M.M., Montone, R.C., 2010. Historical record
1054 of polycyclic aromatic hydrocarbons (PAHs) and spheroidal carbonaceous
1055 particles (SCPs) in marine sediment cores from Admiralty Bay, King
1056 George Island, Antarctica. **Environmental Pollution** 158, 192–200.
1057 doi:10.1016/j.envpol.2009.07.025
1058
1059 Negri, A., Burns, K., Boyle, S., Brinkman, D., Webster, N., 2006.
1060 Contamination in sediments, bivalves and sponges of McMurdo Sound,

1061 Antarctica. **Environmental Pollution** 143, 456–467.
1062 doi:10.1016/j.envpol.2005.12.005
1063
1064 Pereira, W.E., Rostad, C.E., Taylor, H.E., 1980. Mount St. Helens,
1065 Whashington, 1980 volcanic eruption: characterization of organic
1066 compounds in ash samples. **Geophysical Research Letters** 7, 953–954.
1067
1068 Pfeiffer, S., Peter, H., 2004. Ecological studies toward the management of
1069 an Antarctic tourist landing site (Penguin Island, South Shetland Islands)
1070 Ecological studies toward the management of an Antarctic tourist landing
1071 site (Penguin Island, South Shetland Islands). **Polar Record** 40, 1–9.
1072 doi:10.1017/S0032247404003845
1073
1074 Préndez, M., Barra, C., Toledo, C., Richter, P., 2011. Alkanes and
1075 polycyclic aromatic hydrocarbons in marine surficial sediment near
1076 Antarctic stations at Fildes Peninsula, King George Island. **Antarctic**
1077 **Science** 23, 578–588. doi:10.1017/S0954102011000563
1078
1079 Raymond, T., King, C.K., Raymond, B., Stark, J.S., Snape, I., 2016. Oil
1080 Pollution in Antarctica. **Oil Spill Science and Technology: Second**
1081 **Edition**. Elsevier Inc. doi:10.1016/B978-0-12-809413-6.00014-X
1082
1083 Readman, J.W., Fillmann, G., Tolosa, I., Bartocci, J., Villeneuve, J.P.,
1084 Catinni, C., Mee, L.D., 2002. Petroleum and PAH contamination of the
1085 Black Sea. **Marine Pollution Bulletin** 44, 48–62. doi:10.1016/S0025-
1086 326X(01)00189-8
1087
1088 Robbins, J.A., Edgington, D.N., 1975. Determination of recent
1089 sedimentation rates in Lake Michigan using Pb-210 and Cs-137.
1090 **Geochimica et Cosmochimica Acta.** 39, 285–304.
1091
1092 Rowland, S.J., 1990. Production of acyclic isoprenoid hydrocarbons by
1093 laboratory maturation of methanogenic bacteria. **Organic Geochemistry**
1094 15, 9–16. doi:10.1016/0146-6380(90)90181-X
1095
1096 Schwarzbauer, J., Jovančićević B., 2015. Main type of organic matter in
1097 Geosphere. In: Fossil Matter in the Geosphere (Ed. 1). **Fundamentals in**
1098 **Organic Geochemistry**. VIII, 158. doi:10.1007/978-3-319-11938-0
1099
1100 Silliman, J.E., Meyers, P. a., Eadie, B.J., 1998. Perylene: An indicator of
1101 alteration processes or precursor materials?. **Organic Geochemistry** 29,
1102 1737–1744. doi:10.1016/S0146-6380(98)00056-4

Silva, D.A.M., Bícego, M.C., 2010. Polycyclic aromatic hydrocarbons and petroleum biomarkers in São Sebastião Channel, Brazil: Assessment of petroleum contamination. **Marine Environmental Research** 69, 277–286. doi:10.1016/j.marenvres.2009.11.007

Simoneit, B.R.T., Grimalt, J.O., Wang, T.G., 1986. Cyclic terpenoids of contemporary resinous plant detritus and of fossil woods, ambers, coals and petroleums. Workshop on Advances in biomarkers and kerogens I, 71–73.

Simoneit, B.R.T., 1982. Some Applications of Computerized GC-MS to the Determination of Biogenic and Anthropogenic Organic Matter in the Environment. **International Journal of Environmental Analytical Chemistry** 12, 177–193. doi:10.1080/03067318208078326

Smellie, J.L., 2001. Lithostratigraphy and volcanic evolution of Deception Island, South Shetland Islands. **Antarctic Science** 13, 188–209.

Smith JR, K.L., Baldwin, R.J., Kaufmann, R.S., Sturz, A., 2003. Ecosystem studies at Deception Island Antarctica: an overview. **Deep-Sea Research II** 50, 1595–1609. doi:10.1016/S0967-0645(03)00081-X

Snape, I., Harvey, P.M., Ferguson, S.H., Rayner, J.L., Revill, A.T., 2005. Investigation of evaporation and biodegradation of fuel spills in Antarctica I. A chemical approach using GC-FID. **Chemosphere** 61, 1485–1494. doi:10.1016/j.chemosphere.2005.04.108

Soclo, H.H., Garrigues, P.H., Ewald, M., 2000. Origin of Polycyclic Aromatic Hydrocarbons (PAHs) in Coastal Marine Sediments: Case Studies in Cotonou (Benin) and Aquitaine (France) Areas. **Marine Pollution Bulletin** 40, 387–396.

Stortini, A.M., Martellini, T., Del Bubba, M., Lepri, L., Capodaglio, G., Cincinelli, A., 2009. n-Alkanes, PAHs and surfactants in the sea surface microlayer and sea water samples of the Gerlache Inlet sea (Antarctica). **Microchemical Journal** 92, 37–43. doi:10.1016/j.microc.2008.11.005

Stout, S.A., 1992. Aliphatic and aromatic triterpenoid hydrocarbons in a Tertiary angiospermous lignite. **Organic Geochemistry** 18, 51–66. doi:10.1016/0146-6380(92)90143-L

1145 Stout, S.A., Emsbo-mattingly, S.D., 2008. Concentration and character of
1146 PAHs and other hydrocarbons in coals of varying rank – Implications for
1147 environmental studies of soils and sediments containing particulate coal.
1148 **Organic Geochemistry** 39, 801–819.
1149 doi:10.1016/j.orggeochem.2008.04.017
1150
1151 Stracquadanio, M., Dinelli, E., Trombini, C., 2003. Role of Volcanic Dust in
1152 the Atmospheric Transport and Deposition of Polycyclic Aromatic
1153 Hydrocarbons and Mercury. **Journal of Environmental Monitoring** 5,
1154 984–988. doi:10.1039/b308587b
1155
1156 Taniguchi, S., Montone, R.C., Bícego, M.C., Colabuono, F.I., Weber, R.R.,
1157 Sericano, J.L., 2009. Chlorinated pesticides, polychlorinated biphenyls and
1158 polycyclic aromatic hydrocarbons in the fat tissue of seabirds from King
1159 George Island, Antarctica. **Marine Pollution Bulletin** 58, 129–133.
1160 doi:10.1016/j.marpolbul.2008.09.026
1161
1162 Tolosa, I., Mesa-Albernas, M., Alonso-Hernandez, C.M., 2009. Inputs and
1163 sources of hydrocarbons in sediments from Cienfuegos bay, Cuba.
1164 **Marine Pollution Bulletin** 58, 1624–1634.
1165 doi:10.1016/j.marpolbul.2009.07.006
1166
1167 Tolosa, I., Mora, S. De, Reza, M., Villeneuve, J., Bartocci, J., Cattini, C.,
1168 2004. Aliphatic and aromatic hydrocarbons in coastal Caspian Sea
1169 sediments. **Marine Pollution Bulletin** 48, 44–60. doi:10.1016/S0025-
1170 326X(03)00255-8
1171
1172 Venkatesan, M.I., Kaplan, I.R., 1987. The Lipid Geochemistry of Antarctic
1173 Marine Sediments: Bransfield Strait. **Marine Chemistry** 21, 347–375.
1174
1175 Venkatesan, M.I., 1988a. Organic geochemistry of marine sediments in
1176 Antarctic region: Marine lipids in McMurdo Sound. **Organic Geochemistry**
1177 12, 13–27. doi:10.1016/0146-6380(88)90111-8
1178
1179 Venkatesan, M.I., 1988b. Occurrence and possible sources of perylene in
1180 marine sediments-a review. **Marine Chemistry** 25, 1–27.
1181 doi:10.1016/0304-4203(88)90011-4
1182
1183 Volkman, J.K., Holdsworth, D.G., Neill, G.P., Bavor, H.J., 1992.
1184 Identification of natural, anthropogenic and petroleum hydrocarbons in
1185 aquatic sediments. The **Science of the total environment** 112, 203–219.
1186 doi:10.1016/0048-9697(92)90188-X

Wang, T.G., Simoneit, B.R.T., 1991. Organic geochemistry and coal petrology of Tertiary brown coal in the Zhoujing mine, Baise Basin, South China. **Fuel** 70, 819–829. doi:10.1016/0016-2361(91)90188-G

Wang, Z., Fingas, M., Page, D.S., 1999. Oil spill identification. **Journal of Chromatography** A 843, 369–411. doi:10.1016/S0021-9673(99)00120-X

Wang, Z., Stout, S.A., Fingas, M., 2006. Forensic fingerprinting of biomarkers for oil spill characterization and source identification. **Environmental Forensics** 7, 105–146. doi:10.1080/15275920600667104

Wang, Z., et al. 2009 Forensic differentiation of biogenic organic compounds from petroleum hydrocarbons in biogenic and petrogenic compounds cross-contaminated soils and sediments. **Journal of Chromatography A** 1216, 1174-1191.

Wisnieski, E., Cheschim, L.M.M., Martins, C.C., 2016. Validação de um método analítico para determinação de marcadores orgânicos geoquímicos em amostras de sedimentos marinhos. **Química Nova** 8, 1007-1014, doi:10.5935/0100-4042.20160103.

Xue, R., Chen, L., Lu, Z., Wang, J., Yang, H., Zhang, J., Cai, M., 2016. Spatial distribution and source apportionment of PAHs in marine surface sediments of Prydz Bay, East Antarctica. **Environmental Pollution** 219, 528–536. doi:10.1016/j.envpol.2016.05.084

Yang, C. et al. 2011. Fingerprinting Analysis and Characterization of Hydrocarbons in Sediment Cores from the Pearl River Estuary, China**.** **Environmental Forensics**, v. 12, p. 49–62

Yu, Y., Wade, T.L., Fang, J., McDonald, S., Brooks, J.M., 1995. Gas chromatographic-mass spectrometric analysis of polycyclic aromatic hydrocarbon metabolites in Antarctic fish (*Notothenia gibberifrons*) injected with Diesel Fuel Arctic. **Archives of Environmental Contamination and Toxicology** 29, 241–246. doi:10.1007/BF00212975

Yunker, M.B., Macdonald, R.W., Snowdon, L.R., Fowler, B.R., 2011. Organic Geochemistry Alkane and PAH biomarkers as tracers of terrigenous organic carbon in Arctic Ocean sediments. **Organic Geochemistry** 42, 1109–1146. doi:10.1016/j.orggeochem.2011.06.007

1229 Yunker, M.B., Macdonald, R.W., Vingarzan, R., Mitchell, H., Goyette, D.,
1230 Sylvestre, S., 2002. PAHs in the Fraser River basin: a critical appraisal of
1231 PAH ratios as indicators of PAH source and composition. **Organic**
1232 **Geochemistry** 33, 489–515.
1233
1234 Yunker, M.B., Mclaughlin, F.A., Fowler, M.G., Fowler, B.R., 2014. Organic
1235 Geochemistry Source apportionment of the hydrocarbon background in
1236 sediment cores from Hecate Strait, a pristine sea on the west coast of
1237 British Columbia. **Organic Geochemistry** 76, 235–258.
1238 doi:10.1016/j.orggeochem.2014.08.010
1239
1240 Zhang, W., Zhang, S., Wan, C., Yue, D., Ye, Y., Wang, X., 2008. Source
1241 diagnostics of polycyclic aromatic hydrocarbons in urban road runoff, dust,
1242 rain and canopy throughfall. **Environmental Pollution** 153, 594–601.
1243 doi:10.1016/j.envpol.2007.09.004
1244

3. Supplementary Material

TABLE S1. Complete list of PAHs analyzed and individual concentrations (ng g^{-1}) in blank and reference material samples.

PAHs (ng g^{-1})	B01	B02	B03	B04	B05	B06	RM01	RM02	RM03
Naphthalene	<LD	<LD	<LD	<LD	1.47	1.11	10.77	16.23	10.09
Acenaphthylene	<LD	<LD	<LD	<LD	<LD	<LD	2.65	3.74	3.50
Acenaphthene	<LD	<LD	<LD	<LD	<LD	<LD	1.77	1.43	1.70
Fluorene	<LD	<LD	<LD	<LD	<LD	<LD	2.13	2.58	1.82
Dibenzothiophene	<LD	<LD	<LD	<LD	<LD	<LD	0.98	1.12	1.87
Phenanthrene	<LD	<LD	<LD	<LD	<LD	<LD	19.41	20.16	21.52
Anthracene	<LD	<LD	<LD	<LD	<LD	<LD	6.94	6.64	9.04
Fluoranthene	<LD	<LD	<LD	<LD	<LD	<LD	67.99	81.64	68.09
Pyrene	<LD	<LD	<LD	<LD	<LD	<LD	48.14	63.91	49.88
Benz(*a*)anthracene	<LD	<LD	<LD	<LD	<LD	0.72	32.42	46.22	4<LD
Chrysene	<LD	<LD	<LD	<LD	<LD	<LD	33.22	37.05	37.88
Benzo(*b*)fluoranthene	<LD	1.45	1.84	<LD	<LD	3.90	68.43	57.07	36.33
Benzo(*j+k*)fluoranthene	0.74	1.34	2.06	<LD	<LD	3.31	30.22	37.04	26.15
Benzo(*e*)pyrene	<LD	<LD	<LD	<LD	<LD	<LD	77.67	94.96	74.75
Benzo(*a*)pyrene	<LD	1.87	1.92	<LD	<LD	3.86	46.37	45.03	33.23
Indeno [1.2.3-*c,d*]pyrene	<LD	0.82	0.88	<LD	<LD	3.16	38.79	70.94	41.53
Dibenz(*a,h*)anthracene	<LD	<LD	<LD	<LD	<LD	1.87	6.79	13.64	7.43
Benzo(*g,h,*i)perylene	<LD	0.58	0.59	<LD	<LD	2.54	25.52	49.85	26.29
∑-C_1-naphthalene	<LD	<LD	<LD	<LD	<LD	<LD	3.96	4.75	4.14
∑-C_2-naphthalene	<LD	<LD	<LD	<LD	<LD	<LD	13.10	17.05	14.82
∑-C_3-naphthalene	<LD	<LD	<LD	<LD	<LD	<LD	9.10	11.04	7.75
∑-C_1-fluorene	<LD	<LD	<LD	<LD	<LD	<LD	3.22	3.97	2.85
∑-C_2-fluorene	<LD	<LD	<LD	<LD	<LD	<LD	5.56	6.23	3.67
∑-C_1- dibenzothiophene	<LD	<LD	<LD	<LD	<LD	<LD	0.69	0.81	0.96
∑-C_2-dibenzothiophene	<LD	<LD	<LD	<LD	<LD	<LD	<LD	1.61	1.29
∑-C_1-phenanthrene	<LD	<LD	<LD	<LD	<LD	<LD	11.23	13.15	11.28
∑-C_2-phenanthrene	<LD	<LD	<LD	<LD	<LD	<LD	9.72	12.13	7.51
∑-C_1-(fluoranthene+pyrene)	<LD	<LD	<LD	<LD	<LD	<LD	21.33	25.39	17.85
∑-C_1-chrysene	<LD	<LD	<LD	<LD	<LD	<LD	11.99	13.40	11.08
Perylene	<LD	<LD	<LD	<LD	<LD	<LD	201.79	248.18	208.04

<LD: Below limit of detection.

TABLE S2. Complete list of *n*-alkanes analyzed and individual concentrations (μg g^{-1}) in blank samples (<LD: below detection limit).

***n*-alkanes (μg g^{-1})**	**B01**	**B02**	**B03**	**B04**	**B05**	**B06**
n-C_{10}	<LD	<LD	<LD	<LD	<LD	0.032
n-C_{11}	0.042	0.042	0.064	0.061	0.051	<LD
n-C_{12}	<LD	<LD	<LD	<LD	<LD	<LD
n-C_{13}	<LD	<LD	0.007	0.006	<LD	<LD
n-C_{14}	<LD	<LD	0.006	0.009	<LD	<LD
n-C_{15}	<LD	<LD	<LD	<LD	<LD	<LD
n-C_{16}	<LD	<LD	<LD	<LD	<LD	<LD
n-C_{17}	<LD	<LD	<LD	<LD	<LD	<LD
n-C_{18}	<LD	<LD	<LD	<LD	<LD	<LD
n-C_{19}	<LD	<LD	<LD	<LD	<LD	<LD
n-C_{20}	<LD	<LD	<LD	<LD	<LD	<LD
n-C_{21}	<LD	<LD	<LD	<LD	<LD	<LD
n-C_{22}	0.039	0.049	0.038	0.039	0.052	<LD
n-C_{23}	<LD	<LD	<LD	<LD	<LD	<LD
n-C_{24}	<LD	<LD	<LD	<LD	<LD	<LD
n-C_{25}	<LD	<LD	<LD	<LD	<LD	<LD
n-C_{26}	0.015	<LD	<LD	<LD	<LD	<LD
n-C_{27}	0.017	<LD	<LD	<LD	<LD	<LD
n-C_{28}	0.195	<LD	<LD	<LD	<LD	<LD
n-C_{29}	<LD	<LD	<LD	<LD	<LD	<LD
n-C_{30}	<LD	<LD	<LD	<LD	<LD	<LD
n-C_{31}	<LD	<LD	<LD	<LD	<LD	<LD
n-C_{32}	<LD	<LD	<LD	<LD	<LD	<LD
n-C_{33}	<LD	<LD	<LD	<LD	<LD	<LD
n-C_{34}	<LD	<LD	<LD	<LD	<LD	<LD
n-C_{35}	<LD	<LD	<LD	<LD	<LD	<LD
n-C_{36}	<LD	<LD	<LD	<LD	<LD	<LD
n-C_{37}	<LD	<LD	<LD	<LD	<LD	<LD
n-C_{38}	<LD	<LD	<LD	<LD	<LD	<LD
n-C_{39}	<LD	<LD	<LD	<LD	<LD	<LD
n-C_{40}	<LD	<LD	<LD	<LD	<LD	<LD

TABLE S3. Isoprenoids hydrocarbons and aliphatic fraction (in μg g^{-1}), including petroleum biomarkers (in ng g^{-1}) in blank samples.

Samples	B01	B02	B03	B04	B05	B06
Isoprenoids (μg g^{-1})						
Pristane (Pris)	<LD	<LD	<LD	<LD	<LD	<LD
Phytane (Phy)	<LD	<LD	<LD	<LD	<LD	<LD
∑AHs	<LD	2.761	2.231	2.273	2.200	1.485
Resolved AHs	<LD	2.002	1.767	1.764	1.819	1.052
UCM	<LD	<LD	<LD	<LD	<LD	<LD
Petroleum Biomarkers (ng g^{-1})						
C_{20}-Tricyclic terpane	<LD	<LD	<LD	<LD	<LD	<LD
C_{21}-Tricyclic terpane	<LD	<LD	<LD	<LD	<LD	<LD
C_{23}-Tricyclic terpane	<LD	<LD	<LD	<LD	<LD	<LD
C_{24}-Tricyclic terpane	<LD	<LD	<LD	<LD	<LD	<LD
C_{25}-Tricyclic terpane	<LD	<LD	<LD	<LD	<LD	<LD
C_{24}-Tetracyclic terpane	<LD	<LD	<LD	<LD	<LD	<LD
C_{26}-Tricyclic terpane	<LD	<LD	<LD	<LD	<LD	<LD
C_{27}-18α,21β Hopane (Ts)	<LD	<LD	<LD	<LD	<LD	<LD
C_{27}-17α,21β Hopane (Tm)	<LD	<LD	<LD	<LD	<LD	<LD
C_{29}-17α,21β Hopane	<LD	<LD	<LD	<LD	<LD	<LD
C_{30}-17α,21β Hopane	<LD	<LD	<LD	<LD	<LD	<LD
C_{31}-17α,21β Hopane (22S)	<LD	<LD	<LD	<LD	<LD	<LD
C_{31}-17α,21β Hopane (22R)	<LD	<LD	<LD	<LD	<LD	<LD
C_{30}-17β,21β Hopane	<LD	<LD	<LD	<LD	<LD	<LD
C_{32}-17α,21β Hopane (22S)	<LD	<LD	<LD	<LD	<LD	<LD
C_{32}-17α,21β Hopane (22R)	<LD	<LD	<LD	<LD	<LD	<LD

<LD: Below limit of detection.

TABLE S4. Parameters and diagnostic ratios of PAHs (ng g^{-1}), AHs (µg g^{-1}) and PBMs (ng g^{-1}) in PGI-1 core.

Depth (cm)	**0 - 2**	**2 - 3**	**3 - 4**	**4 - 5**	**5 - 6**	**6 - 7**	**7 - 8**	**8 - 9**	**9-10**	**10-11**	**11-12**	**12-13**	**13-14**	**14-16**
Estimated date	**2007-1985**	**1985-1974**	**1974-1963**	**1963-1953**	**1953-1941**	**1941-1930**	**1930-1919**	**1919-1908**	**1908-1897**	**1897-1886**	**1886-1875**	**1876-1864**	**1864-1953**	**1853-1831**
∑PAHs	45.66	55.99	15.26	13.20	13.67	13.69	19.80	19.01	15.55	20.66	26.37	20.32	19.07	18.82
∑Alkylated PAHs	11.68	14.35	8.28	8.19	9.92	9.73	9.83	6.76	11.51	14.33	17.20	14.41	13.89	14.82
∑2-3 rings PAHs	2.51	6.03	2.80	2.42	2.54	2.35	2.79	6.67	2.61	3.92	4.08	3.69	3.09	2.33
∑4-6 rings PAHs	31.47	35.61	4.18	2.59	1.21	1.61	7.18	5.58	1.43	2.41	5.09	2.22	2.09	1.67
Perylene	3.37	3.31	4.36	4.14	4.31	5.48	5.89	4.84	4.94	6.52	9.02	11.9	11.44	9.95
%Perylene/5rings PAHs	17.9	49.0	76.2	84.6	86.9	84.0	64.1	77.5	86.0	80.8	82.3	88.8	89.6	91.9
BaA/228	0.50	0.52	nc	nc	nc	nc	0.41	0.45	nc	nc	nc	nc	nc	nc
IP/IP+Bghi	0.51	0.55	0.51	0.48	nc	nc	0.52	nc	nc	nc	nc	nc	nc	nc
C_0-P/(∑C_0+C_1)-P	0.49	0.61	0.62	0.56	0.59	0.49	0.57	0.72	0.50	0.58	0.49	0.55	0.47	0.42
∑AHs	10.66	13.39	9.52	9.68	8.23	9.31	10.59	5.35	6.23	7.31	9.16	9.25	6.17	6.41
UCM	4.79	4.66	5.01	5.15	3.79	4.16	5.47	3.42	3.63	4.16	3.98	5.39	3.34	4.27
Total *n*-alkanes	2.22	0.45	0.64	0.64	0.67	0.60	0.64	0.66	0.81	0.98	1.08	1.01	1.11	0.77
n-C_{15}+*n*-C_{17}+*n*-C_{19}	0.31	0.13	0.23	0.18	0.23	0.17	0.21	0.17	0.28	0.36	0.34	0.37	0.22	0.24
Odd/even (<*n*-C_{24})	1.07	1.39	1.08	1.04	1.03	1.07	1.02	1.14	1.14	1.09	1.06	1.11	1.11	1.14
Odd/even(>*n*-C_{23})	1.12	1.29	1.42	1.09	1.56	1.26	1.27	1.53	1.36	1.66	0.96	1.49	1.23	1.32
UCM/total *n*-alkanes	2.16	10.32	7.80	8.05	5.63	6.89	8.55	5.18	4.48	4.24	3.68	5.36	3.01	5.55
CPI_1	1.24	1.94	1.74	1.27	1.89	1.49	1.47	1.74	1.62	1.93	1.04	1.76	1.35	1.50
CPI_2	1.07	1.35	1.07	1.02	1.03	1.04	1.01	1.02	1.06	1.08	1.05	1.09	1.05	1.10
Pristane	0.11	0.06	0.08	0.05	0.07	0.05	0.07	0.05	0.10	0.10	0.10	0.10	0.06	0.07
Phytane	0.08	0.05	0.07	0.05	0.07	0.04	0.06	0.04	0.08	0.11	0.09	0.10	0.05	0.06
Total terpanes	2.81	<LD	4.41	6.02	5.58	8.39	5.60	5.25	3.96	32.6	10.5	20.2	4.49	6.50
Total hopanes	< LD	< LD	< LD	< LD	< LD	< LD	< LD	< LD	< LD	< LD	< LD	< LD	< LD	0.53

<LD: below limit of detection. nc: not calculated (individual compounds < LD).

TABLE S5. Parameters and diagnostic ratios of PAHs (ng g^{-1}), AHs (µg g^{-1}) and PBMs (ng g^{-1}) in PGI-2 core.

Depth (cm)	0 - 2	2 - 3	3 - 4	4 - 5	5 - 6	6 - 7	7 - 8	8 - 9	9-10	10-11	11-12	12-13	13-14	14-15	15-16	16-18
Estimated date	**2007 - 1999**	**1999 - 1995**	**1995 - 1991**	**1991 - 1987**	**1987 - 1983**	**1983 - 1979**	**1979 - 1975**	**1975 - 1971**	**1971 - 1967**	**1967 - 1963**	**1963 - 1959**	**1959 - 1955**	**1955 - 1951**	**1951 - 1947**	**1947 - 1943**	**1943 - 1935**
∑PAHs	40.53	45.60	36.37	60.34	35.55	31.49	31.10	34.22	35.52	31.95	32.65	31.15	27.84	30.73	24.70	23.28
∑Alkylated PAHs	27.82	33.64	26.55	53.20	27.38	25.11	24.56	26.73	28.86	23.74	24.00	23.50	22.57	24.32	20.29	17.53
∑2-3 rings PAHs	9.50	8.77	6.98	4.02	5.01	4.09	4.16	4.70	3.32	3.69	4.69	4.43	2.86	4.17	2.04	3.85
∑4-6 rings PAHs	3.21	3.19	2.84	3.12	3.16	2.29	2.38	2.79	3.34	4.52	3.96	3.22	2.41	2.24	2.37	1.90
Perylene	5.22	5.40	4.13	5.48	5.04	5.48	5.13	4.86	5.14	4.77	4.31	4.1	3.26	3.49	3.10	3.18
%Perylene/5rings PAHs	77.5	79.1	76.0	78.6	76.7	81.3	79.4	75.2	76.7	75.4	77.6	73.6	67.0	72.1	73.8	74.3
BaA/228	0.33	0.29	0.36	0.32	0.32	nc	nc	nc	nc	nc	nc	nc	nc	nc	nc	nc
IP/IP+Bghi	nc	nc	nc	nc	nc	nc	nc	nc	nc	0.48	0.48	nc	nc	nc	nc	nc
C_0-P/(∑C_0+C_1)-P	0.62	0.64	0.64	0.42	0.53	0.43	0.42	0.52	0.38	0.43	0.55	0.55	0.47	0.59	0.58	0.56
∑AHs	9.89	11.97	8.86	7.10	7.94	9.61	8.81	11.31	7.06	5.64	6.04	5.57	8.14	8.64	21.91	6.29
UCM	2.01	3.68	2.57	2.91	4.06	5.64	5.14	7.25	3.22	1.77	2.01	2.01	3.76	3.91	9.06	2.49
Total *n*-alkanes	0.81	0.85	0.43	1.02	1.01	1.04	0.90	0.99	0.84	0.80	0.74	0.79	1.12	1.24	0.85	0.72
n-C_{15}+*n*-C_{17}+*n*-C_{19}	0.15	0.18	0.11	0.25	0.25	0.26	0.22	0.33	0.22	0.20	0.18	0.19	0.17	0.25	0.18	0.17
Odd/even (<*n*-C_{24})	0.92	0.89	1.53	0.93	0.93	0.97	0.96	0.95	0.87	0.86	0.84	0.85	0.73	0.83	0.92	0.95
Odd/even(>*n*-C_{23})	0.81	1.06	1.18	1.09	1.14	1.17	1.30	1.61	1.69	1.53	1.49	1.15	1.14	1.14	1.09	1.15
UCM/total *n*-alkanes	2.47	4.36	6.01	2.86	4.03	5.41	5.69	7.35	3.82	2.21	2.71	2.56	3.37	3.15	10.71	3.46
CPI_1	0.90	1.24	1.63	1.52	1.66	1.79	1.80	2.26	2.03	1.89	1.87	1.37	1.18	1.25	1.26	1.39
CPI_2	1.00	0.97	1.72	0.92	0.93	0.95	1.03	0.95	0.85	0.89	0.88	0.90	0.78	0.87	0.95	1.00
Pristane	0.06	0.07	0.06	0.08	0.07	0.09	0.07	0.12	0.07	0.07	0.06	0.06	0.05	0.08	0.07	0.05
Phytane	0.02	0.02	0.01	0.07	0.07	0.08	0.07	0.07	0.06	0.05	0.05	0.05	0.05	0.08	0.06	0.04
Total terpanes	<LD	<LD	<LD	8.70	14.8	15.0	12.1	8.69	6.33	5.66	6.58	3.94	3.10	3.21	2.40	2.44
Total hopanes	< LD	< LD	< LD	< LD	< LD	< LD	< LD	< LD	< LD	< LD	< LD	< LD	< LD	< LD	< LD	< LD

<LD: below limit of detection. nc: not calculated (individual compounds < LD).

TABLE S6. Parameters and diagnostic ratios of PAHs (ng g^{-1}), AHs (µg g^{-1}) and PBMs (ng g^{-1}) in DCP-1 sediment core.

Depth (cm)	**0 - 2**	**2 - 3**	**3 - 4**	**4 - 5**	**5 - 6**	**6 - 7**	**7 - 8**	**8 - 9**	**9-10**
Estimated date	**2007-1998**	**1998-1993**	**1993-1988**	**1988-1983**	**1983-1979**	**1979-1974**	**1974-1969**	**1969-1965**	**1965-1960**
∑PAHs	22.76	26.84	14.06	13.46	12.37	10.18	8.54	12.17	7.68
∑Alkylated PAHs	12.48	15.27	10.06	9.72	9.13	6.76	5.05	5.70	4.33
∑2-3 rings PAHs	2.63	6.12	0.99	1.34	<LD	<LD	0.82	<LD	<LD
∑4-6 rings PAHs	7.65	5.45	3.01	2.40	3.24	3.42	2.67	6.47	3.35
Perylene	<LD	<LD	<LD	<LD	<LD	<LD	<LD	<LD	<LD
BaA/228	nc	0.43	nc	nc	nc	nc	0.43	0.38	0.42
IP/IP+Bghi	0.51	nc	nc	0.60	0.56	0.59	nc	1.00	nc
C_0-P/(∑C_0+C_1)-P	0.61	0.45	0.48	0.54	nc	nc	0.59	nc	nc
∑AHs	19.01	13.80	15.70	8.80	8.47	6.27	6.45	12.17	9.51
UCM	12.18	8.76	7.08	6.03	5.72	4.28	4.26	9.15	6.46
Total *n*-alkanes	2.48	1.22	1.13	0.58	0.59	0.26	0.47	0.47	0.48
n-C_{15}+*n*-C_{17}+*n*-C_{19}	0.17	0.21	0.12	0.11	0.13	0.08	0.10	0.10	0.09
Odd/even (<*n*-C_{24})	0.52	0.56	0.42	0.60	0.73	0.55	0.65	0.46	0.61
Odd/even(>*n*-C_{23})	0.46	0.98	1.32	1.00	0.89	0.00	0.93	1.35	1.00
UCM/total *n*-alkanes	4.91	7.16	6.24	10.44	9.71	16.71	9.15	19.39	13.48
CPI_1	0.56	1.22	1.35	1.13	0.86	1.33	1.39	1.17	1.16
CPI_2	0.57	0.63	0.54	0.64	0.71	0.60	0.67	0.57	0.67
Pristane	0.07	0.09	0.05	0.05	0.05	0.03	0.04	0.05	0.05
Phytane	0.05	0.07	0.03	0.03	0.03	0.02	0.03	0.04	0.04
Total terpanes	1.48	5.75	4.00	4.41	4.77	4.22	3.54	6.85	7.14
Total hopanes	<LD	<LD	0.51	<LD	<LD	<LD	0.50	8.47	2.81

<LD: below limit of detection. nc: not calculated (individual compounds < LD).

TABLE S7. Sum parameters and diagnostic ratios of PAHs (ng g^{-1}), AHs (µg g^{-1}) and PBMs (ng g^{-1}) in DCP-2 sediment core and in DCP-3 (surficial sample).

Depth (cm)	0 - 1	1-2	2 - 3	3 - 4	4 - 5	5 - 6	6 - 7	7 - 8	8 - 9	9-10	DCP-3
Estimated date	**2007-2001**	**2001-1995**	**1995-1989**	**1989-1983**	**1983-1977**	**1977-1971**	**1971-1965**	**1965-1959**	**1959-1953**	**1953-1947**	
∑PAHs	19.57	14.31	2.01	na	10.96	19.04	12.09	5.55	7.19	6.80	3.75
∑Alkylated PAHs	15.61	11.47	1.32	na	7.45	9.51	8.36	2.98	3.93	3.64	3.75
∑2-3 rings PAHs	3.38	2.27	0.00	na	1.76	5.88	2.27	0.71	0.73	0.84	<LD
∑4-6 rings PAHs	0.58	0.57	0.69	na	1.75	3.65	1.46	1.86	2.53	2.32	<LD
Perylene	<LD	<LD	<LD	na	<LD	<LD	<LD	<LD	<LD	<LD	<LD
BaA/228	nc	nc	nc	nc	nc	nc	nc	nc	nc	nc	nc
IP/IP+Bghi	nc	nc	1.00	nc	nc	nc	nc	nc	nc	nc	nc
C_0-P/(∑C_0+C_1)-P	0.52	0.00	nc	nc	0.60	0.53	0.59	nc	nc	0.61	nc
∑AHs	6.71	5.82	8.36	5.27	5.80	8.67	4.50	6.14	7.09	7.77	4.63
UCM	4.05	3.59	6.12	3.51	3.33	5.53	2.28	3.34	5.23	3.20	3.07
Total *n*-alkanes	0.34	0.43	0.64	0.30	0.27	2.29	0.25	0.32	0.31	0.29	0.31
n-C_{15}+*n*-C_{17}+*n*-C_{19}	0.05	0.11	0.14	0.08	0.09	0.10	0.08	0.08	0.07	0.08	0.08
Odd/even (<*n*-C_{24})	1.06	0.94	1.00	0.92	0.91	0.94	0.90	0.95	0.93	1.01	0.87
Odd/even(>*n*-C_{23})	1.13	1.06	0.95	1.12	1.20	0.35	1.21	0.84	0.83	0.93	1.03
UCM/total *n*-alkanes	11.77	8.30	9.51	11.91	12.44	2.41	9.21	10.47	16.98	11.05	9.86
CPI_1	1.19	1.45	1.16	1.46	1.46	0.70	1.56	1.04	0.94	1.14	1.51
CPI_2	1.00	0.90	0.91	0.89	0.91	0.82	0.87	0.89	0.88	0.96	0.89
Pristane	0.06	0.04	0.05	0.03	0.04	0.03	0.03	0.03	0.03	0.04	0.03
Phytane	0.05	0.01	0.02	0.01	0.01	0.02	0.01	0.01	0.04	0.04	0.03
Total terpanes	29.6	22.0	34.9	27.4	29.1	29.8	35.45	12.5	17.0	21.6	0.65
Total hopanes	16.8	8.8	11.6	11.9	15.1	11.8	22.10	4.32	15.7	5.36	< LD

na: not available. <LD: below limit of detection. nc: not calculated (individual compounds < LD).

Fig.S1. Grain size distribution profiles in DCP-1, DCP-2, PGI-1 and PGI-2 sediment cores.

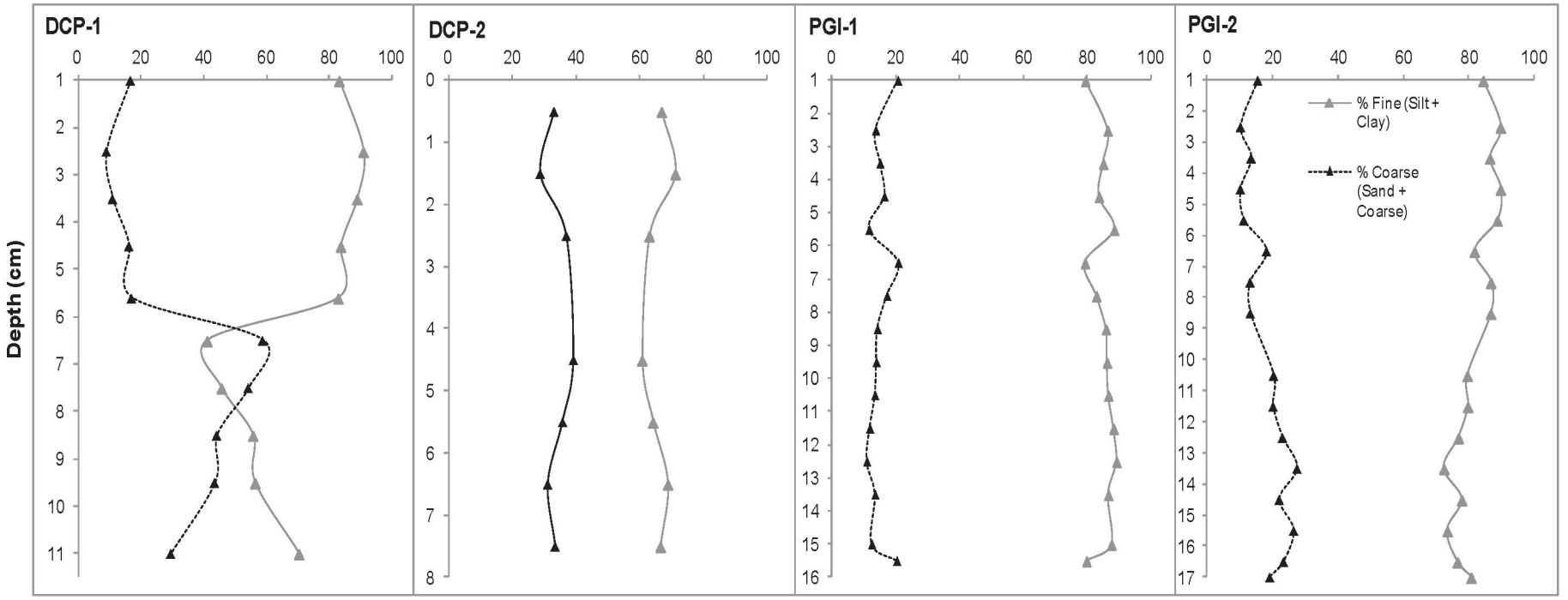

Fig.S2. Concentration profiles for alkyl, 2-3 rings and 4-6 rings PAHs in DCP-1, DCP-2, PGI-1 and PGI-2 sediment cores.

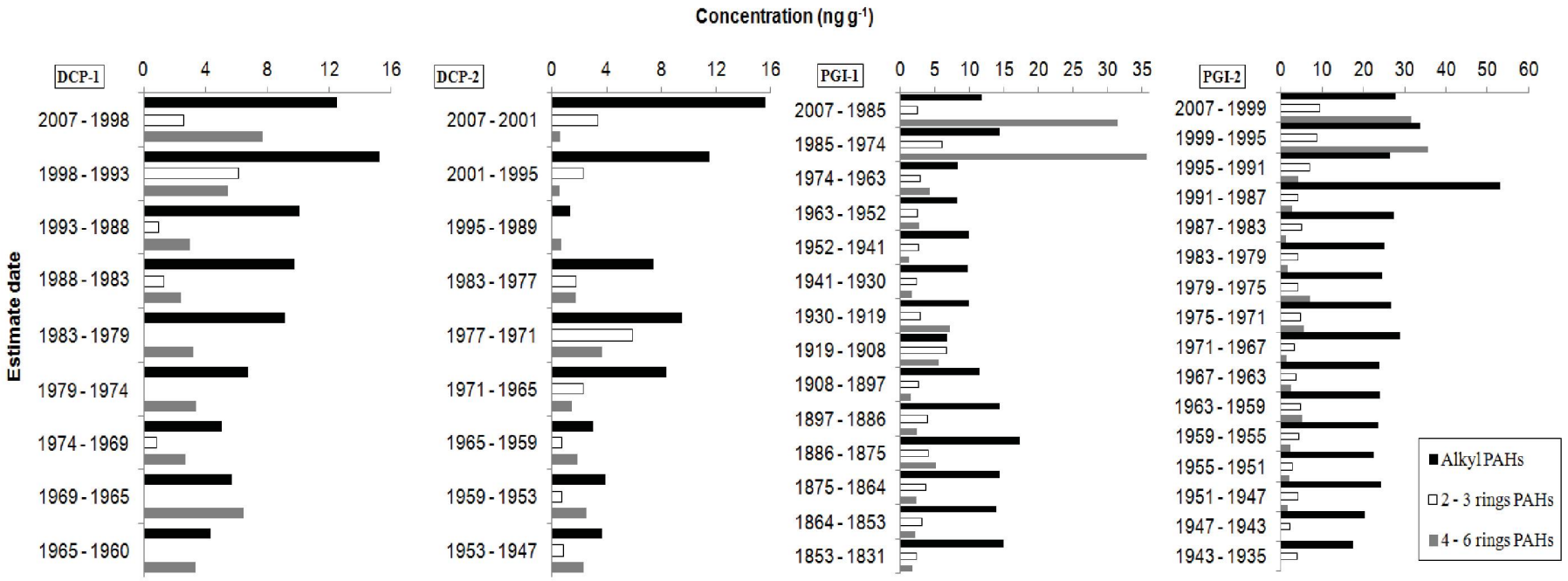

4. Anexos – Dados Brutos

Anexo 1. Concentrações em ng g^{-1} de hidrocarbonetos policíclicos aromáticos no testemunho PGI-1.

Profundidade (cm)	0 - 2	2 - 3	3 - 4	4 - 5	5 - 6	6 - 7	7 - 8	8 - 9	9-10	10-11	11-12	12-13	13-14	14-16
Data estimada	**2007 1985**	**1985 1974**	**1974 1963**	**1963 1953**	**1953 1941**	**1941 1930**	**1930 1919**	**1919 1908**	**1908 1897**	**1897 1886**	**1886 1875**	**1876 1864**	**1864 1953**	**1853 1831**
Naftaleno	0,92	1,03	0,91	1,01	0,90	0,99	0,88	0,92	1,05	1,01	1,25	1,03	1,28	1,04
Acenafitleno	<LD	<LD	<LD	<LD	<LD	<LD	<LD	<LD	<LD	<LD	<LD	<LD	<LD	<LD
Acenafteno	<LD	<LD	<LD	<LD	<LD	<LD	<LD	<LD	<LD	<LD	<LD	<LD	<LD	<LD
Fluoreno	<LD	<LD	<LD	<LD	<LD	<LD	<LD	<LD	<LD	<LD	0,58	<LD	<LD	<LD
Dibenzotiofeno	<LD	<LD	<LD	<LD	<LD	<LD	<LD	<LD	<LD	<LD	<LD	<LD	<LD	<LD
Fenantreno	1,59	4,27	1,89	1,41	1,64	1,36	1,91	2,51	1,56	2,91	2,25	2,66	1,81	1,29
Antraceno	<LD	0,73	<LD	<LD	<LD	<LD	<LD	3,24	<LD	<LD	<LD	<LD	<LD	<LD
Fluroanteno	<LD	7,57	<LD	<LD	<LD	<LD	<LD	1,68	<LD	<LD	<LD	<LD	<LD	<LD
Pireno	<LD	8,10	<LD	<LD	<LD	<LD	<LD	<LD	<LD	<LD	2,35	<LD	<LD	<LD
Benzo(*a*)antraceno	0,65	7,25	<LD	<LD	<LD	<LD	0,56	0,88	<LD	<LD	<LD	<LD	<LD	<LD
Criseno	0,66	6,79	0,97	0,70	0,56	0,57	0,79	1,08	0,63	0,87	0,81	0,73	0,77	0,80
benzo(*b*)fluoranteno	3,44	1,89	<LD	<LD	<LD	<LD	1,59	<LD	<LD	<LD	<LD	<LD	<LD	<LD
benzo(*j+k*)fluoranteno	2,20	<LD	<LD	<LD	<LD	<LD	<LD	<LD	<LD	<LD	<LD	<LD	<LD	<LD
benzo(*e*)pireno	0,82	0,81	0,81	0,75	0,65	1,04	0,78	0,74	0,80	0,83	1,93	0,94	1,32	0,87
benzo(*a*)pireno	3,86	<LD	<LD	<LD	<LD	<LD	<LD	<LD	<LD	<LD	<LD	<LD	<LD	<LD
indeno[1,2,3-*c,d*]pireno	7,50	1,36	0,94	<LD	<LD	<LD	1,32	<LD	<LD	<LD	<LD	<LD	<LD	<LD
dibenzo(*a,h*)antraceno	5,05	0,74	0,55	<LD	<LD	<LD	0,92	0,66	<LD	0,71	<LD	0,55	<LD	<LD
benzo(*g,h,*i)perileno	7,29	1,10	0,91	0,59	<LD	<LD	1,22	0,54	<LD	<LD	<LD	<LD	<LD	<LD
∑-C_1-naftaleno	1,49	2,92	0,93	1,44	1,44	1,42	0,85	0,88	1,63	1,91	2,14	1,82	2,14	2,02
∑-C_2-naftaleno	2,07	2,51	2,30	2,51	2,55	2,21	2,42	2,13	2,64	2,93	3,33	2,92	3,33	3,80
∑-C_3-naftaleno	2,49	2,47	1,85	1,73	2,36	1,92	2,65	1,62	2,76	3,67	4,17	3,26	2,38	3,63
∑-C_1-fluoreno	1,17	1,25	1,04	0,81	0,98	0,74	1,04	0,59	1,40	1,71	1,79	1,49	0,97	1,09
∑-C_2- fluoreno	1,61	0,75	0,99	<LD	0,86	0,78	0,83	0,56	0,99	1,09	1,63	1,22	1,42	1,19
∑-C_1- dibenzotiofeno	<LD	<LD	<LD	<LD	<LD	<LD	<LD	<LD	<LD	<LD	<LD	<LD	<LD	<LD
∑-C_2-dibenzotiofeno	<LD	<LD	<LD	<LD	<LD	<LD	<LD	<LD	<LD	<LD	<LD	<LD	<LD	<LD
∑-C_1-fenantreno	1,65	2,76	1,17	1,13	1,15	1,40	1,45	0,98	1,57	2,10	2,37	2,14	2,01	1,77
∑-C_2-fenantreno	0,67	1,15	<LD	0,57	0,58	0,69	0,59	<LD	0,52	0,92	1,05	0,95	0,86	0,75
∑-C_1-(fluoranteno+pireno)	0,53	0,54	<LD	<LD	<LD	0,57	<LD	<LD	<LD	<LD	0,72	0,61	0,78	0,57
∑-C_1-criseno	<LD	<LD	<LD	<LD	<LD	<LD	<LD	<LD	<LD	<LD	<LD	<LD	<LD	<LD
Perileno	3,37	3,31	4,36	4,14	4,31	5,48	5,89	4,84	4,94	6,52	9,02	11,9	11,44	9,95

<LD: Abaixo do limite de detecção.

Anexo 2. Concentrações em ng g^{-1} de hidrocarbonetos policíclicos aromáticos no testemunho PGI-2.

Profundidade (cm)	0 - 2	2 - 3	3 - 4	4 - 5	5 - 6	6 - 7	7 - 8	8 - 9	9-10	10-11	11-12	12-13	13-14	14-15	15-16	16-18
Data estimada	**2007**	**1999**	**1995**	**1991**	**1987**	**1983**	**1979**	**1975**	**1971**	**1967**	**1963**	**1959**	**1955**	**1951**	**1947**	**1943**
	1999	**1995**	**1991**	**1987**	**1983**	**1979**	**1975**	**1971**	**1967**	**1963**	**1959**	**1955**	**1951**	**1947**	**1943**	**1935**
Naftaleno	3,12	2,67	2,39	2,21	2,37	2,35	2,45	2,27	2,06	2,42	2,41	2,33	1,69	1,93	<LD	2,13
Acenafitleno	<LD	<LD	<LD	<LD	<LD	<LD	<LD	<LD	<LD	<LD	<LD	<LD	<LD	<LD	<LD	<LD
Acenafteno	<LD	<LD	<LD	<LD	<LD	<LD	<LD	<LD	<LD	<LD	<LD	<LD	<LD	<LD	<LD	<LD
Fluoreno	0,67	0,56	<LD	<LD	<LD	<LD	<LD	<LD	<LD	<LD	<LD	<LD	<LD	<LD	<LD	<LD
Dibenzotiofeno	<LD	<LD	<LD	<LD	<LD	<LD	<LD	<LD	<LD	<LD	<LD	<LD	<LD	<LD	<LD	<LD
Fenantreno	5,71	5,54	4,59	1,81	2,64	1,74	1,71	2,43	1,26	1,27	2,28	2,10	1,17	2,24	2,04	1,72
Antraceno	<LD	<LD	<LD	<LD	<LD	<LD	<LD	<LD	<LD	<LD	<LD	<LD	<LD	<LD	<LD	<LD
Fluroanteno	<LD	<LD	<LD	<LD	<LD	<LD	<LD	<LD	<LD	<LD	<LD	<LD	<LD	<LD	<LD	<LD
Pireno	<LD	<LD	<LD	<LD	<LD	<LD	<LD	<LD	<LD	<LD	<LD	<LD	<LD	<LD	<LD	<LD
Benzo(*a*)antraceno	0,56	0,51	0,56	0,52	0,52	<LD	<LD	<LD	<LD	<LD	<LD	<LD	<LD	<LD	<LD	<LD
Criseno	1,14	1,26	0,98	1,11	1,11	1,03	1,05	1,19	1,02	1,18	1,08	1,13	0,81	0,89	0,69	0,80
benzo(*b*)fluoranteno	<LD	<LD	<LD	<LD	<LD	<LD	<LD	<LD	<LD	<LD	<LD	<LD	<LD	<LD	<LD	<LD
benzo(*j+k*)fluoranteno	<LD	<LD	<LD	<LD	<LD	<LD	<LD	<LD	<LD	<LD	<LD	<LD	<LD	<LD	<LD	<LD
benzo(*e*)pireno	1,51	1,42	1,30	1,49	1,53	1,26	1,33	1,60	1,56	1,55	1,24	1,46	1,60	1,35	1,10	1,10
benzo(*a*)pireno	<LD	<LD	<LD	<LD	<LD	<LD	<LD	<LD	<LD	<LD	<LD	<LD	<LD	<LD	<LD	<LD
indeno[1,2,3-*c,d*]pireno	<LD	<LD	<LD	<LD	<LD	<LD	<LD	<LD	<LD	0,86	0,78	<LD	<LD	<LD	<LD	<LD
dibenzo(*a,h*)antraceno	<LD	<LD	<LD	<LD	<LD	<LD	<LD	<LD	<LD	<LD	<LD	<LD	<LD	<LD	<LD	<LD
benzo(*g,h,*i)perileno	<LD	<LD	<LD	<LD	<LD	<LD	<LD	<LD	0,76	0,93	0,86	0,63	<LD	<LD	0,58	<LD
∑-C_1-naftaleno	6,04	8,02	6,40	9,95	6,20	5,54	5,58	5,81	5,96	6,41	6,28	6,04	4,87	5,52	4,07	5,03
∑-C_2-naftaleno	7,31	11,65	8,06	19,57	8,01	6,50	6,65	7,50	9,72	7,66	7,48	7,60	8,16	8,88	7,24	5,84
∑-C_3-naftaleno	4,93	6,33	4,61	14,05	4,30	4,76	4,09	5,28	5,66	3,80	3,53	3,68	4,86	4,99	4,22	2,65
∑-C_1-fluoreno	1,39	1,16	1,03	1,48	1,39	1,38	1,13	1,29	1,22	0,98	1,06	1,01	0,84	0,94	0,79	0,60
∑-C_2- fluoreno	1,37	0,86	0,93	2,42	1,91	1,89	1,77	1,74	1,44	1,13	1,44	1,12	1,09	0,91	0,95	0,67
∑-C_1- dibenzotiofeno	<LD	<LD	<LD	<LD	<LD	<LD	<LD	<LD	<LD	<LD	<LD	<LD	<LD	<LD	<LD	<LD
∑-C_2-dibenzotiofeno	<LD	<LD	<LD	<LD	<LD	<LD	<LD	<LD	<LD	<LD	<LD	<LD	<LD	<LD	<LD	<LD
∑-C_1-fenantreno	3,51	3,07	2,62	2,49	2,31	2,28	2,32	2,21	2,09	1,70	1,85	1,72	1,34	1,53	1,50	1,37
∑-C_2-fenantreno	1,38	1,12	1,15	1,36	1,43	1,22	1,23	1,22	1,11	0,75	0,92	0,95	0,70	0,79	0,77	0,72
∑-C_1-(fluoranteno+pireno)	1,22	0,84	1,15	1,17	1,14	0,89	1,15	1,02	1,00	0,65	0,90	0,83	0,71	0,76	0,75	0,65
∑-C_1-criseno	0,67	0,59	0,60	0,71	0,69	0,65	0,64	0,66	0,66	0,66	0,54	0,55	<LD	<LD	<LD	<LD
Perileno	5,22	5,40	4,13	5,48	5,04	5,48	5,13	4,86	5,14	4,77	4,31	4,1	3,26	3,49	3,10	3,18

<LD: Abaixo do limite de detecção.

Anexo 3. Concentrações em ng g^{-1} de hidrocarbonetos policíclicos aromáticos no testemunho DCP-1.

Profundidade (cm)	0 - 2	2 - 3	3 - 4	4 - 5	5 - 6	6 - 7	7 - 8	8 - 9	9-10
Data estimada	2007 1998	1998 1993	1993 1988	1988 1983	1983 1979	1979 1974	1974 1969	1969 1965	1965 1960
Naftaleno	<LD	4,71	<LD	<LD	<LD	<LD	<LD	<LD	<LD
Acenafitleno	<LD	<LD	<LD	<LD	<LD	<LD	<LD	<LD	<LD
Acenafteno	<LD	<LD	<LD	<LD	<LD	<LD	<LD	<LD	<LD
Fluoreno	<LD	<LD	<LD	<LD	<LD	<LD	<LD	<LD	<LD
Dibenzotiofeno	<LD	<LD	<LD	<LD	<LD	<LD	<LD	<LD	<LD
Fenantreno	2,63	1,41	0,99	1,34	<LD	<LD	0,82	<LD	<LD
Antraceno	<LD	<LD	<LD	<LD	<LD	<LD	<LD	<LD	<LD
Fluroanteno	<LD	1,92	<LD	<LD	<LD	<LD	<LD	<LD	<LD
Pireno	<LD	1,94	<LD	<LD	<LD	<LD	<LD	<LD	<LD
Benzo(*a*)antraceno	<LD	0,69	<LD	<LD	<LD	<LD	0,79	1,00	0,99
Criseno	<LD	0,90	1,15	0,86	0,90	0,86	1,04	1,62	1,35
benzo(*b*)fluoranteno	1,82	<LD	<LD	<LD	<LD	<LD	<LD	1,78	<LD
benzo(*j+k*)fluoranteno	1,55	<LD	0,85	<LD	<LD	<LD	<LD	<LD	<LD
benzo(*e*)pireno	<LD	<LD	1,01	<LD	<LD	<LD	0,84	1,38	1,01
benzo(*a*)pireno	1,95	<LD	<LD	<LD	<LD	<LD	<LD	<LD	<LD
indeno[1,2,3-*c,d*]pireno	0,89	<LD	<LD	0,92	0,99	1,11	<LD	0,69	<LD
dibenzo(*a,h*)antraceno	0,60	<LD	<LD	<LD	0,58	0,69	<LD	<LD	<LD
benzo(*g,h,*i)perileno	0,84	<LD	<LD	0,62	0,77	0,76	<LD	<LD	<LD
$\sum$-C_1-naftaleno	1,44	1,60	0,74	0,85	0,65	0,57	<LD	<LD	<LD
$\sum$-C_2-naftaleno	3,73	4,21	3,37	3,24	2,99	2,55	2,07	2,12	1,80
$\sum$-C_3-naftaleno	2,24	2,30	1,65	1,39	1,42	1,03	1,18	1,09	0,74
$\sum$-C_1-fluoreno	1,28	0,74	0,61	0,96	1,07	0,74	<LD	<LD	<LD
$\sum$-C_2- fluoreno	1,29	2,29	1,27	1,46	1,38	1,20	0,64	0,67	0,99
$\sum$-C_1- dibenzotiofeno	<LD	<LD	<LD	<LD	<LD	<LD	<LD	<LD	<LD
$\sum$-C_2-dibenzotiofeno	<LD	<LD	<LD	<LD	<LD	<LD	<LD	<LD	<LD
$\sum$-C_1-fenantreno	1,70	1,73	1,09	1,14	1,03	0,67	0,57	0,52	<LD
$\sum$-C_2-fenantreno	0,80	1,53	0,70	0,68	0,59	<LD	<LD	<LD	<LD
$\sum$-C_1-(fluoranteno+pireno)	<LD	0,87	0,63	<LD	<LD	<LD	0,59	0,74	0,80
$\sum$-C_1-criseno	<LD	<LD	<LD	<LD	<LD	<LD	<LD	0,56	<LD
Perileno	<LD	<LD	<LD	<LD	<LD	<LD	<LD	<LD	<LD

<LD: Abaixo do limite de detecção.

Anexo 4. Concentrações em ng g^{-1} de hidrocarbonetos policíclicos aromáticos no testemunho DCP-2.

Profundidade (cm)	0 - 1	1-2	2 - 3	4 - 5	5 - 6	6 - 7	7 - 8	8 - 9	9-10	DCP-3
Data estimada	2007	2001	1995	1983	1977	1971	1965	1959	1953	
	2001	1995	1989	1977	1971	1965	1959	1953	1947	
Naftaleno	1,42	2,27	<LD	<LD	4,51	1,11	0,71	0,73	<LD	<LD
Acenafitleno	<LD	<LD	<LD	<LD	<LD	<LD	<LD	<LD	<LD	<LD
Acenafteno	<LD	<LD	<LD	<LD	<LD	<LD	<LD	<LD	<LD	<LD
Fluoreno	<LD	<LD	<LD	<LD	<LD	<LD	<LD	<LD	<LD	<LD
Dibenzotiofeno	<LD	<LD	<LD	<LD	<LD	<LD	<LD	<LD	<LD	<LD
Fenantreno	1,96	<LD	<LD	1,76	1,37	1,16	<LD	<LD	0,84	<LD
Antraceno	<LD	<LD	<LD	<LD	<LD	<LD	<LD	<LD	0<LD	<LD
Fluroanteno	<LD	<LD	<LD	<LD	1,68	<LD	<LD	<LD	<LD	<LD
Pireno	<LD	<LD	<LD	<LD	<LD	<LD	<LD	<LD	<LD	<LD
Benzo(*a*)antraceno	<LD	<LD	<LD	<LD	<LD	<LD	<LD	<LD	<LD	<LD
Criseno	0,58	0,57	<LD	1,01	1,05	0,86	1,00	1,42	1,33	<LD
benzo(*b*)fluoranteno	<LD	<LD	<LD	<LD	<LD	<LD	<LD	<LD	<LD	<LD
benzo(*j+k*)fluoranteno	<LD	<LD	<LD	<LD	<LD	<LD	<LD	<LD	<LD	<LD
benzo(*e*)pireno	<LD	<LD	<LD	0,74	0,92	0,60	0,86	1,11	0,99	<LD
benzo(*a*)pireno	<LD	<LD	<LD	<LD	<LD	<LD	<LD	<LD	<LD	<LD
indeno[1,2,3-*c,d*]pireno	<LD	<LD	0,69	<LD	<LD	<LD	<LD	<LD	<LD	<LD
dibenzo(*a,h*)antraceno	<LD	<LD	<LD	<LD	<LD	<LD	<LD	<LD	<LD	<LD
benzo(*g,h,*i)perileno	<LD	<LD	<LD	<LD	<LD	<LD	<LD	<LD	<LD	<LD
∑-C_1-naftaleno	1,46	0,60	<LD	<LD	0,64	0,64	<LD	<LD	<LD	<LD
∑-C_2-naftaleno	2,72	1,82	0,73	1,17	1,65	1,82	0,86	0,91	0,75	0,93
∑-C_3-naftaleno	3,38	1,54	0,59	1,12	1,63	1,70	0,89	0,80	0,63	0,63
∑-C_1-fluoreno	1,61	1,73	<LD	0,79	1,39	1,19	<LD	<LD	<LD	0,59
∑-C_2- fluoreno	3,45	3,56	<LD	1,76	1,71	1,55	0,67	0,96	1,07	0,85
∑-C_1- dibenzotiofeno	<LD	<LD	<LD	<LD	<LD	<LD	<LD	<LD	<LD	<LD
∑-C_2-dibenzotiofeno	<LD	<LD	<LD	<LD	<LD	<LD	<LD	<LD	<LD	<LD
∑-C_1-fenantreno	1,82	2,22	<LD	1,19	1,22	0,82	0,56	0,53	0,54	0,75
∑-C_2-fenantreno	1,17	<LD	<LD	0,82	0,73	0,64	<LD	<LD	<LD	<LD
∑-C_1-(fluoranteno+pireno)	<LD	<LD	<LD	0,60	0,54	<LD	<LD	0,73	0,65	<LD
∑-C_1-criseno	<LD	<LD	<LD	<LD	<LD	<LD	<LD	<LD	<LD	<LD
Perileno	<LD	<LD	<LD	<LD	<LD	<LD	<LD	<LD	<LD	<LD

<LD: Abaixo do limite de detecção.

Anexo 5. Concentrações de *n*-alcanos em μg g^{-1} no testemunho PGI-1 (<LD: Abaixo do limite de detecção).

Profundidade (cm)	0 - 2	2 - 3	3 - 4	4 - 5	5 - 6	6 - 7	7 - 8	8 - 9	9-10	10-11	11-12	12-13	13-14	14-16
Data estimada	**2007 1985**	**1985 1974**	**1974 1963**	**1963 1953**	**1953 1941**	**1941 1930**	**1930 1919**	**1919 1908**	**1908 1897**	**1897 1886**	**1886 1875**	**1876 1864**	**1864 1953**	**1853 1831**
n-C_{10}	<LD	<LD	<LD	<LD	<LD	<LD	<LD	0,010	0,008	<LD	<LD	<LD	<LD	<LD
n-C_{11}	<LD	<LD	<LD	<LD	<LD	<LD	<LD	0,033	0,024	<LD	<LD	0,006	<LD	<LD
n-C_{12}	0,009	0,009	0,008	0,009	0,008	<LD	0,008	0,008	0,007	0,009	0,011	<LD	0,010	0,010
n-C_{13}	0,016	0,017	0,013	0,015	0,014	0,014	0,014	0,015	0,014	0,016	0,018	0,019	0,016	0,014
n-C_{14}	0,021	0,021	0,027	0,033	0,028	0,037	0,029	0,035	0,024	0,028	0,036	0,030	0,043	0,030
n-C_{15}	0,054	0,048	0,053	0,050	0,060	0,052	0,057	0,059	0,062	0,074	0,081	0,080	0,067	0,067
n-C_{16}	0,132	0,033	0,096	0,075	0,100	0,065	0,091	0,078	0,123	0,148	0,143	0,150	0,087	0,101
n-C_{17}	0,189	0,054	0,123	0,088	0,121	0,079	0,101	0,079	0,154	0,197	0,180	0,202	0,102	0,121
n-C_{18}	0,130	0,065	0,091	0,071	0,092	0,061	0,083	0,058	0,114	0,158	0,138	0,153	0,082	0,089
n-C_{19}	0,062	0,027	0,054	0,046	0,047	0,039	0,048	0,036	0,063	0,091	0,076	0,084	0,055	0,052
n-C_{20}	0,019	<LD	0,016	0,019	0,015	0,025	0,018	0,017	0,022	0,025	0,027	0,031	0,018	0,018
n-C_{21}	0,019	0,031	0,017	0,021	0,018	0,022	0,017	0,017	0,020	0,025	0,027	0,026	0,023	0,020
n-C_{22}	0,024	0,015	0,018	0,027	0,026	0,023	0,022	0,020	0,018	0,023	0,028	0,030	0,030	0,012
n-C_{23}	0,020	0,022	0,017	0,024	0,017	0,020	0,018	0,019	0,022	0,022	0,024	0,022	0,036	0,023
n-C_{24}	0,025	0,024	0,014	0,019	0,015	0,020	0,014	0,015	0,016	0,015	0,022	0,018	0,039	0,020
n-C_{25}	0,064	0,021	0,021	0,029	0,024	0,023	0,024	0,024	0,021	0,023	0,035	0,029	0,065	0,033
n-C_{26}	0,089	0,007	<LD	0,004	0,005	0,007	0,004	0,018	0,013	0,018	0,027	0,021	0,059	0,020
n-C_{27}	0,171	0,009	0,010	0,016	0,013	0,015	0,010	0,034	0,023	0,030	0,045	0,032	0,080	0,036
n-C_{28}	0,193	0,017	0,018	0,023	0,017	0,024	0,015	0,022	0,016	0,014	0,075	0,017	0,062	0,032
n-C_{29}	0,240	0,020	0,020	0,024	0,026	0,029	0,023	0,030	0,023	0,032	0,035	0,026	0,076	0,031
n-C_{30}	0,182	<LD	0,013	0,031	0,013	0,023	0,026	0,015	0,013	0,015	0,015	0,013	0,051	0,020
n-C_{31}	0,181	0,012	0,013	0,015	0,015	0,026	0,018	0,019	0,012	0,018	0,029	0,016	0,056	0,021
n-C_{32}	0,125	<LD	<LD	<LD	<LD	<LD	<LD	<LD	<LD	<LD	0,011	<LD	0,030	<LD
n-C_{33}	0,090	<LD	<LD	<LD	<LD	<LD	<LD	<LD	<LD	<LD	<LD	<LD	0,020	<LD
n-C_{34}	0,058	<LD	<LD	<LD	<LD	<LD	<LD	<LD	<LD	<LD	<LD	<LD	<LD	<LD
n-C_{35}	0,038	<LD	<LD	<LD	<LD	<LD	<LD	<LD	<LD	<LD	<LD	<LD	<LD	<LD
n-C_{36}	0,033	<LD	<LD	<LD	<LD	<LD	<LD	<LD	<LD	<LD	<LD	<LD	<LD	<LD
n-C_{37}	0,018	<LD	<LD	<LD	<LD	<LD	<LD	<LD	<LD	<LD	<LD	<LD	<LD	<LD
n-C_{38}	0,014	<LD	<LD	<LD	<LD	<LD	<LD	<LD	<LD	<LD	<LD	<LD	<LD	<LD
n-C_{39}	<LD	<LD	<LD	<LD	<LD	<LD	<LD	<LD	<LD	<LD	<LD	<LD	<LD	<LD
n-C_{40}	<LD	<LD	<LD	<LD	<LD	<LD	<LD	<LD	<LD	<LD	<LD	<LD	<LD	<LD

Anexo 6. Concentrações de *n*-alcanos em μg g^{-1} no testemunho PGI-2 (<LD: Abaixo do limite de detecção).

Profundidade (cm)	0 - 2	2 - 3	3 - 4	4 - 5	5 - 6	6 - 7	7 - 8	8 - 9	9-10	10-11	11-12	12-13	13-14	14-15	15-16	16-18
Data estimada	2007 1999	1999 1995	1995 1991	1991 1987	1987 1983	1983 1979	1979 1975	1975 1971	1971 1967	1967 1963	1963 1959	1959 1955	1955 1951	1951 1947	1947 1943	1943 1935
n-C_{10}	0,014	<LD	<LD	<LD	<LD	0,013	0,017	<LD	<LD	0,013	0,012	0,012	<LD	<LD	<LD	<LD
n-C_{11}	0,020	<LD	<LD	0,009	0,010	0,021	0,013	<LD	0,012	0,023	0,021	0,017	<LD	0,010	<LD	<LD
n-C_{12}	0,053	0,050	0,035	0,043	0,052	0,049	0,051	0,023	0,030	0,048	0,048	0,048	0,028	0,038	0,044	0,047
n-C_{13}	0,059	0,087	0,045	0,083	0,080	0,054	0,056	0,032	0,073	0,072	0,073	0,078	0,068	0,084	0,055	0,055
n-C_{14}	0,079	0,135	0,021	0,127	0,117	0,078	0,067	0,064	0,160	0,097	0,101	0,099	0,133	0,136	0,067	0,068
n-C_{15}	0,067	0,084	0,048	0,080	0,079	0,074	0,063	0,098	0,094	0,076	0,068	0,073	0,071	0,079	0,058	0,061
n-C_{16}	0,052	0,059	0,029	0,100	0,108	0,114	0,077	0,160	0,107	0,098	0,085	0,091	0,083	0,107	0,076	0,066
n-C_{17}	0,056	0,058	0,039	0,120	0,123	0,126	0,110	0,170	0,092	0,092	0,077	0,086	0,068	0,121	0,085	0,071
n-C_{18}	0,052	0,054	0,028	0,090	0,087	0,096	0,079	0,122	0,048	0,065	0,052	0,059	0,048	0,084	0,067	0,047
n-C_{19}	0,029	0,034	0,023	0,047	0,049	0,063	0,051	0,059	0,033	0,030	0,030	0,031	0,030	0,049	0,035	0,035
n-C_{20}	0,008	0,006	<LD	0,020	0,023	0,028	0,023	0,027	0,016	0,012	0,020	0,019	0,015	0,022	0,014	0,020
n-C_{21}	0,027	0,031	0,024	0,023	0,026	0,030	0,027	0,024	0,016	0,014	0,015	0,014	0,014	0,020	0,017	0,016
n-C_{22}	0,043	0,051	0,018	0,052	0,048	0,049	0,054	0,037	0,029	0,043	0,037	0,041	0,063	0,079	0,032	0,027
n-C_{23}	0,018	0,021	0,022	0,040	0,037	0,047	0,033	0,030	0,019	0,016	0,015	0,016	0,018	0,025	0,026	0,024
n-C_{24}	0,025	0,022	0,019	0,038	0,037	0,047	0,034	0,024	0,012	0,013	0,012	0,013	0,020	0,028	0,030	0,024
n-C_{25}	0,024	0,019	0,019	0,037	0,033	0,043	0,037	0,029	0,019	0,017	0,016	0,014	0,042	0,033	0,037	0,027
n-C_{26}	0,031	0,025	0,012	0,019	0,018	0,022	0,019	0,018	0,016	0,014	0,012	0,013	0,044	0,036	0,034	0,021
n-C_{27}	0,033	0,028	0,019	0,023	0,021	0,026	0,030	0,028	0,023	0,019	0,019	0,021	0,064	0,047	0,051	0,028
n-C_{28}	0,034	0,022	0,013	0,016	0,012	0,012	0,014	0,012	0,014	0,013	0,011	0,010	0,057	0,047	0,022	0,023
n-C_{29}	0,029	0,029	0,014	0,020	0,022	0,025	0,020	0,020	0,020	0,016	0,017	0,019	0,068	0,064	0,027	0,027
n-C_{30}	0,026	0,016	<LD	0,014	0,011	0,011	0,012	<LD	<LD	<LD	<LD	0,011	0,055	0,042	0,030	0,016
n-C_{31}	0,020	0,014	<LD	0,015	0,013	0,014	0,016	0,010	0,009	0,009	<LD	<LD	0,050	0,044	0,026	0,015
n-C_{32}	0,015	<LD	<LD	<LD	<LD	<LD	<LD	<LD	<LD	<LD	<LD	<LD	0,033	0,028	0,013	<LD
n-C_{33}	<LD	<LD	<LD	<LD	<LD	<LD	<LD	<LD	<LD	<LD	<LD	<LD	0,020	0,019	<LD	<LD
n-C_{34}	<LD	<LD	<LD	<LD	<LD	<LD	<LD	<LD	<LD	<LD	<LD	<LD	0,014	<LD	<LD	<LD
n-C_{35}	<LD	<LD	<LD	<LD	<LD	<LD	<LD	<LD	<LD	<LD	<LD	<LD	0,010	<LD	<LD	<LD
n-C_{36}	<LD	<LD	<LD	<LD	<LD	<LD	<LD	<LD	<LD	<LD	<LD	<LD	<LD	<LD	<LD	<LD
n-C_{37}	<LD	<LD	<LD	<LD	<LD	<LD	<LD	<LD	<LD	<LD	<LD	<LD	<LD	<LD	<LD	<LD
n-C_{38}	<LD	<LD	<LD	<LD	<LD	<LD	<LD	<LD	<LD	<LD	<LD	<LD	<LD	<LD	<LD	<LD
n-C_{39}	<LD	<LD	<LD	<LD	<LD	<LD	<LD	<LD	<LD	<LD	<LD	<LD	<LD	<LD	<LD	<LD
n-C_{40}	<LD	<LD	<LD	<LD	<LD	<LD	<LD	<LD	<LD	<LD	<LD	<LD	<LD	<LD	<LD	<LD

Anexo 7. Concentrações de *n*-alcanos em μg g^{-1} no testemunho DCP-1 (<LD: Abaixo do limite de detecção).

Profundidade (cm)	0 - 2	2 - 3	3 - 4	4 - 5	5 - 6	6 - 7	7 - 8	8 - 9	9-10
Data estimada	2007 1998	1998 1993	1993 1988	1988 1983	1983 1979	1979 1974	1974 1969	1969 1965	1965 1960
n-C_{10}	<LD	<LD	<LD	<LD	<LD	<LD	<LD	<LD	<LD
n-C_{11}	<LD	<LD	<LD	<LD	<LD	<LD	<LD	<LD	<LD
n-C_{12}	0,009	0,007	0,006	0,010	<LD	<LD	<LD	<LD	<LD
n-C_{13}	0,015	0,014	0,015	0,013	0,007	0,007	0,005	<LD	<LD
n-C_{14}	0,067	0,076	0,064	0,049	0,045	0,044	0,041	0,034	0,025
n-C_{15}	0,055	0,042	0,032	0,027	0,026	0,023	0,022	0,019	0,013
n-C_{16}	0,081	0,082	0,059	0,058	0,059	0,047	0,042	0,041	0,032
n-C_{17}	0,093	0,112	0,067	0,064	0,069	0,046	0,049	0,056	0,053
n-C_{18}	0,107	0,110	0,056	0,054	0,055	0,038	0,046	0,049	0,048
n-C_{19}	0,020	0,059	0,021	0,021	0,031	0,015	0,027	0,022	0,029
n-C_{20}	0,048	0,062	0,015	0,015	0,025	0,011	0,022	0,008	0,026
n-C_{21}	0,022	0,035	<LD	0,007	0,016	<LD	0,016	<LD	0,012
n-C_{22}	0,126	0,218	0,145	0,057	0,061	0,025	0,065	0,104	0,073
n-C_{23}	0,022	0,051	0,011	0,014	0,029	<LD	0,023	0,011	0,018
n-C_{24}	0,089	0,061	0,012	0,020	0,033	<LD	0,028	0,017	0,020
n-C_{25}	0,040	0,053	0,016	0,029	0,025	0,006	0,022	0,024	0,014
n-C_{26}	0,114	0,043	0,023	0,021	0,015	0,009	0,012	0,019	0,013
n-C_{27}	0,083	0,044	0,018	0,018	0,013	0,009	0,011	0,010	0,014
n-C_{28}	0,189	0,044	0,175	0,020	0,017	0,014	0,016	0,019	0,022
n-C_{29}	0,129	0,047	0,263	0,027	0,019	0,016	0,019	0,021	0,023
n-C_{30}	0,158	0,032	0,035	0,022	0,021	<LD	<LD	0,018	0,021
n-C_{31}	0,084	0,031	0,041	0,021	<LD	<LD	<LD	0,019	0,024
n-C_{32}	0,143	<LD	0,032	0,012	<LD	<LD	<LD	<LD	<LD
n-C_{33}	0,062	<LD	0,029	<LD	<LD	<LD	<LD	<LD	<LD
n-C_{34}	0,133	<LD	<LD	<LD	<LD	<LD	<LD	<LD	<LD
n-C_{35}	0,052	<LD	<LD	<LD	<LD	<LD	<LD	<LD	<LD
n-C_{36}	0,130	<LD	<LD	<LD	<LD	<LD	<LD	<LD	<LD
n-C_{37}	0,058	<LD	<LD	<LD	<LD	<LD	<LD	<LD	<LD
n-C_{38}	0,133	<LD	<LD	<LD	<LD	<LD	<LD	<LD	<LD
n-C_{39}	0,067	<LD	<LD	<LD	<LD	<LD	<LD	<LD	<LD
n-C_{40}	0,149	<LD	<LD	<LD	<LD	<LD	<LD	<LD	<LD

Anexo 8. Concentrações de *n*-alcanos em μg g^{-1} no testemunho DCP-2 e na amostra DCP-3 (<LD: Abaixo do limite de detecção).

Profundidade (cm)	0 - 1	1-2	2 - 3	3 - 4	4 - 5	5 - 6	6 - 7	7 - 8	8 - 9	9-10	DCP-3
Data estimada	2007 2001	2001 1995	1995 1989	1989 1983	1983 1977	1977 1971	1971 1965	1965 1959	1959 1953	1953 1947	
n-C_{10}	<LD	<LD	<LD	<LD	<LD	<LD	<LD	<LD	<LD	<LD	0,008
n-C_{11}	<LD	<LD	<LD	<LD	<LD	<LD	<LD	<LD	<LD	<LD	<LD
n-C_{12}	<LD	<LD	<LD	<LD	<LD	<LD	<LD	<LD	<LD	<LD	0,007
n-C_{13}	0,005	0,005	<LD	0,006	<LD	<LD	0,005	<LD	<LD	<LD	<LD
n-C_{14}	0,007	0,015	0,010	0,013	0,007	0,014	0,014	0,007	0,007	<LD	0,006
n-C_{15}	0,011	0,023	0,019	0,019	0,015	0,019	0,019	0,011	0,011	0,008	0,020
n-C_{16}	0,016	0,050	0,045	0,038	0,039	0,039	0,036	0,023	0,024	0,028	0,037
n-C_{17}	0,026	0,058	0,075	0,045	0,054	0,050	0,039	0,041	0,036	0,043	0,038
n-C_{18}	0,020	0,057	0,078	0,039	0,043	0,050	0,037	0,043	0,040	0,040	0,037
n-C_{19}	0,011	0,030	0,050	0,017	0,023	0,026	0,018	0,025	0,024	0,026	0,025
n-C_{20}	0,012	0,024	0,035	0,013	0,014	0,021	0,010	0,019	0,011	0,018	0,018
n-C_{21}	0,008	0,024	0,023	0,010	0,008	0,015	0,008	0,012	0,008	0,013	0,013
n-C_{22}	0,013	0,022	0,034	0,013	0,014	0,023	0,011	0,018	0,016	0,018	0,014
n-C_{23}	0,011	0,018	0,034	0,010	0,007	0,027	0,008	0,015	0,012	0,015	0,014
n-C_{24}	0,010	0,022	0,037	0,013	0,006	0,034	0,007	0,018	0,014	0,013	0,018
n-C_{25}	0,014	0,028	0,029	0,017	0,005	0,026	0,005	0,014	0,020	0,012	0,022
n-C_{26}	0,016	0,017	0,021	0,011	0,006	0,040	0,005	0,010	0,018	0,007	0,012
n-C_{27}	0,021	0,013	0,023	0,010	0,007	0,021	0,007	0,011	0,014	0,008	0,009
n-C_{28}	0,027	0,013	0,027	0,010	0,008	0,040	0,007	0,011	0,016	0,009	0,007
n-C_{29}	0,037	0,014	0,036	0,011	0,012	0,026	0,011	0,010	0,012	0,011	0,007
n-C_{30}	0,027	<LD	0,022	<LD	<LD	0,044	<LD	0,013	0,012	0,013	<LD
n-C_{31}	0,025	<LD	0,018	<LD	<LD	0,163	<LD	0,013	0,008	0,008	<LD
n-C_{32}	0,016	<LD	0,016	<LD	<LD	0,421	<LD	0,005	0,005	<LD	<LD
n-C_{33}	0,011	<LD	0,011	<LD	<LD	0,170	<LD	<LD	<LD	<LD	<LD
n-C_{34}	<LD	<LD	<LD	<LD	<LD	0,042	<LD	<LD	<LD	<LD	<LD
n-C_{35}	<LD	<LD	<LD	<LD	<LD	0,115	<LD	<LD	<LD	<LD	<LD
n-C_{36}	<LD	<LD	<LD	<LD	<LD	0,419	<LD	<LD	<LD	<LD	<LD
n-C_{37}	<LD	<LD	<LD	<LD	<LD	<LD	<LD	<LD	<LD	<LD	<LD
n-C_{38}	<LD	<LD	<LD	<LD	<LD	0,448	<LD	<LD	<LD	<LD	<LD
n-C_{39}	<LD	<LD	<LD	<LD	<LD	<LD	<LD	<LD	<LD	<LD	<LD
n-C_{40}	<LD	<LD	<LD	<LD	<LD	<LD	<LD	<LD	<LD	<LD	<LD

Anexo 9. Concentrações de terpanos e hopanos em ng g^{-1} no testemunho PGI-1.

Profundidade (cm)	0 - 2	2 - 3	3 - 4	4 - 5	5 - 6	6 - 7	7 - 8	8 - 9	9-10	10-11	11-12	12-13	13-14	14-16
Data estimada	**2007 1985**	**1985 1974**	**1974 1963**	**1963 1953**	**1953 1941**	**1941 1930**	**1930 1919**	**1919 1908**	**1908 1897**	**1897 1886**	**1886 1875**	**1876 1864**	**1864 1953**	**1853 1831**
C_{20}-Terpano tricíclico	0,66	< LD	0,80	0,89	0,97	1,22	0,92	0,83	0,65	28,2	5,23	13,1	< LD	0,91
C_{21}-Terpano tricíclico	0,87	< LD	1,20	1,50	1,44	2,27	1,39	1,42	0,92	1,27	1,51	1,93	1,19	1,53
C_{23}-Terpano tricíclico	1,28	< LD	1,64	2,44	2,17	3,29	2,16	2,02	1,58	2,12	2,54	3,45	2,25	2,61
C_{24}-Terpano tricíclico	0,00	< LD	0,77	1,19	1,00	1,61	1,13	0,98	0,81	1,01	1,18	1,67	1,05	1,45
C_{25}-Terpano tricíclico	< LD	< LD	< LD	< LD	< LD	< LD	< LD	< LD	< LD	< LD	< LD	< LD	< LD	< LD
C_{24}-Terpano tricíclico	< LD	< LD	< LD	< LD	< LD	< LD	< LD	< LD	< LD	< LD	< LD	< LD	< LD	< LD
C_{26}-Terpano tricíclico	< LD	< LD	< LD	< LD	< LD	< LD	< LD	< LD	< LD	< LD	< LD	< LD	< LD	< LD
C_{27}-18α,21β Hopano (Ts)	< LD	< LD	< LD	< LD	< LD	< LD	< LD	< LD	< LD	< LD	< LD	< LD	< LD	< LD
C_{27}-17α,21β Hopano (Tm)	< LD	< LD	< LD	< LD	< LD	< LD	< LD	< LD	< LD	< LD	< LD	< LD	< LD	0,53
C_{29}-17α,21β Hopano	< LD	< LD	< LD	< LD	< LD	< LD	< LD	< LD	< LD	< LD	< LD	< LD	< LD	< LD
C_{30}-17α,21β Hopano	< LD	< LD	< LD	< LD	< LD	< LD	< LD	< LD	< LD	< LD	< LD	< LD	< LD	< LD
C_{31}-17α,21β Hopano (22S)	< LD	< LD	< LD	< LD	< LD	< LD	< LD	< LD	< LD	< LD	< LD	< LD	< LD	< LD
C_{31}-17α,21β Hopano (22R)	< LD	< LD	< LD	< LD	< LD	< LD	< LD	< LD	< LD	< LD	< LD	< LD	< LD	< LD
C_{30}-17β,21β Hopano	< LD	< LD	< LD	< LD	< LD	< LD	< LD	< LD	< LD	< LD	< LD	< LD	< LD	< LD
C_{32}-17α,21β Hopano (22S)	< LD	< LD	< LD	< LD	< LD	< LD	< LD	< LD	< LD	< LD	< LD	< LD	< LD	< LD
C_{32}-17α,21β Hopano (22R)	< LD	< LD	< LD	< LD	< LD	< LD	< LD	< LD	< LD	< LD	< LD	< LD	< LD	< LD

<LD: Abaixo do limite de detecção.

Anexo 10. Concentrações de terpanos e hopanos em ng g^{-1} no testemunho PGI-2.

Profundidade (cm)	0 - 2	2 - 3	3 - 4	4 - 5	5 - 6	6 - 7	7 - 8	8 - 9	9-10	10-11	11-12	12-13	13-14	14-15	15-16	16-18
Data estimada	2007 1999	1999 1995	1995 1991	1991 1987	1987 1983	1983 1979	1979 1975	1975 1971	1971 1967	1967 1963	1963 1959	1959 1955	1955 1951	1951 1947	1947 1943	1943 1935
C_{20}-Terpano tricíclico	< LD	< LD	< LD	1,19	2,05	1,92	2,01	1,60	1,40	1,30	1,24	0,95	0,79	0,73	0,56	0,62
C_{21}-Terpano tricíclico	< LD	< LD	< LD	2,31	3,69	3,36	3,01	2,49	2,09	1,65	1,94	1,41	1,11	1,05	0,81	0,74
C_{23}-Terpano tricíclico	< LD	< LD	< LD	3,56	5,10	5,43	4,80	3,16	2,03	1,74	2,35	1,58	1,20	1,43	1,03	1,08
C_{24}-Terpano tricíclico	< LD	< LD	< LD	1,64	2,42	2,55	2,25	1,44	0,81	0,97	1,05	< LD	< LD	< LD	< LD	< LD
C_{25}-Terpano tricíclico	< LD	< LD	< LD	<LD	1,56	1,70	< LD	< LD	< LD	< LD	< LD	< LD	< LD	< LD	< LD	< LD
C_{24}-Terpano tricíclico	< LD	< LD	< LD	< LD	< LD	< LD	< LD	< LD	< LD	< LD	< LD	< LD	< LD	< LD	< LD	< LD
C_{26}-Terpano tricíclico	< LD	< LD	< LD	< LD	< LD	< LD	< LD	< LD	< LD	< LD	< LD	< LD	< LD	< LD	< LD	< LD
C_{27}-18α,21β Hopano (Ts)	< LD	< LD	< LD	< LD	< LD	< LD	< LD	< LD	< LD	< LD	< LD	< LD	< LD	< LD	< LD	< LD
C_{27}-17α,21β Hopano (Tm)	< LD	< LD	< LD	< LD	< LD	< LD	< LD	< LD	< LD	< LD	< LD	< LD	< LD	< LD	< LD	< LD
C_{29}-17α,21β Hopano	< LD	< LD	< LD	< LD	< LD	< LD	< LD	< LD	< LD	< LD	< LD	< LD	< LD	< LD	< LD	< LD
C_{30}-17α,21β Hopano	< LD	< LD	< LD	< LD	< LD	< LD	< LD	< LD	< LD	< LD	< LD	< LD	< LD	< LD	< LD	< LD
C_{31}-17α,21β Hopano (22S)	< LD	< LD	< LD	< LD	< LD	< LD	< LD	< LD	< LD	< LD	< LD	< LD	< LD	< LD	< LD	< LD
C_{31}-17α,21β Hopano (22R)	< LD	< LD	< LD	< LD	< LD	< LD	< LD	< LD	< LD	< LD	< LD	< LD	< LD	< LD	< LD	< LD
C_{30}-17β,21β Hopano	< LD	< LD	< LD	< LD	< LD	< LD	< LD	< LD	< LD	< LD	< LD	< LD	< LD	< LD	< LD	< LD
C_{32}-17α,21β Hopano (22S)	< LD	< LD	< LD	< LD	< LD	< LD	< LD	< LD	< LD	< LD	< LD	< LD	< LD	< LD	< LD	< LD
C_{32}-17α,21β Hopano (22R)	< LD	< LD	< LD	< LD	< LD	< LD	< LD	< LD	< LD	< LD	< LD	< LD	< LD	< LD	< LD	< LD

<LD: Abaixo do limite de detecção.

Anexo 11. Concentrações de terpanos e hopanos em ng g^{-1} no testemunho DCP-1.

Profundidade (cm)	0 - 2	2 - 3	3 - 4	4 - 5	5 - 6	6 - 7	7 - 8	8 - 9	9-10
Data estimada	2007 1998	1998 1993	1993 1988	1988 1983	1983 1979	1979 1974	1974 1969	1969 1965	1965 1960
C_{20}-Terpano tricíclico	< LD	0,63	0,51	0,67	0,67	0,65	< LD	0,60	0,72
C_{21}-Terpano tricíclico	0,56	1,35	0,99	1,15	1,19	1,03	0,85	1,38	1,62
C_{23}-Terpano tricíclico	0,92	2,50	1,62	1,74	1,94	1,68	1,78	3,19	3,12
C_{24}-Terpano tricíclico	< LD	1,27	0,88	0,85	0,97	0,86	0,91	1,68	1,68
C_{25}-Terpano tricíclico	< LD	< LD	< LD	< LD	< LD	< LD	< LD	< LD	< LD
C_{24}-Terpano tricíclico	< LD	< LD	< LD	< LD	< LD	< LD	< LD	< LD	< LD
C_{26}-Terpano tricíclico	< LD	< LD	< LD	< LD	< LD	< LD	< LD	< LD	< LD
C_{27}-18α,21β Hopano (Ts)	< LD	< LD	< LD	< LD	< LD	< LD	< LD	1,03	< LD
C_{27}-17α,21β Hopano (Tm)	<LD	<LD	0,51	<LD	<LD	<LD	0,50	1,14	0,62
C_{29}-17α,21β Hopano	<LD	<LD	<LD	<LD	<LD	<LD	<LD	2,88	<LD
C_{30}-17α,21β Hopano	<LD	<LD	<LD	<LD	<LD	<LD	<LD	3,42	2,19
C_{31}-17α,21β Hopano (22S)	< LD	< LD	< LD	< LD	< LD	< LD	< LD	< LD	< LD
C_{31}-17α,21β Hopano (22R)	< LD	< LD	< LD	< LD	< LD	< LD	< LD	< LD	< LD
C_{30}-17β,21β Hopano	< LD	< LD	< LD	< LD	< LD	< LD	< LD	< LD	< LD
C_{32}-17α,21β Hopano (22S)	< LD	< LD	< LD	< LD	< LD	< LD	< LD	< LD	< LD
C_{32}-17α,21β Hopano (22R)	< LD	< LD	< LD	< LD	< LD	< LD	< LD	< LD	< LD

<LD: Abaixo do limite de detecção.

Anexo 12. Concentrações de terpanos e hopanos em ng g^{-1} no testemunho DCP-2 e na amostra de sedimento superficial (DCP-3).

Profundidade (cm)	0 - 1	1-2	2 - 3	3 - 4	4 - 5	5 - 6	6 - 7	7 - 8	8 - 9	9-10	DCP-3
Data estimada	2007 2001	2001 1995	1995 1989	1989 1983	1983 1977	1977 1971	1971 1965	1965 1959	1959 1953	1953 1947	
C_{20}-Terpano tricíclico	3,96	2,90	3,47	3,98	3,49	3,85	4,83	1,37	1,44	2,45	< LD
C_{21}-Terpano tricíclico	6,34	4,67	7,30	6,02	5,92	6,20	7,32	2,75	2,95	4,46	0,65
C_{23}-Terpano tricíclico	8,75	6,34	11,5	7,83	8,62	9,33	10,8	4,42	5,46	6,97	< LD
C_{24}-Terpano tricíclico	4,02	3,24	5,39	3,82	4,61	4,52	5,55	2,26	2,85	3,65	< LD
C_{25}-Terpano tricíclico	3,32	2,42	3,65	2,84	3,46	3,18	3,90	1,69	2,32	2,35	< LD
C_{24}-Terpano tricíclico	2,29	1,74	2,54	2,10	1,96	1,82	1,87	<LD	1,19	1,02	< LD
C_{26}-Terpano tricíclico	0,97	0,69	1,02	0,79	0,99	0,88	1,16	<LD	0,79	0,65	< LD
C_{27}-18α,21β Hopano (Ts)	2,01	1,37	1,59	1,61	1,63	1,40	2,11	1,03	2,02	0,84	< LD
C_{27}-17α,21β Hopano (Tm)	2,46	1,48	1,93	1,99	2,26	1,97	2,72	0,99	2,19	1,51	< LD
C_{29}-17α,21β Hopano	6,35	2,85	3,59	3,63	5,69	4,07	6,31	0,00	5,18	0,00	< LD
C_{30}-17α,21β Hopano	5,96	3,10	4,47	4,64	5,57	4,35	7,06	2,30	6,31	3,01	< LD
C_{31}-17α,21β Hopano (22S)	<LD	<LD	<LD	<LD	<LD	<LD	1,88	<LD	<LD	<LD	< LD
C_{31}-17α,21β Hopano (22R)	<LD	<LD	<LD	<LD	<LD	<LD	2,01	<LD	<LD	<LD	< LD
C_{30}-17β,21β Hopano	<LD	<LD	<LD	<LD	<LD	<LD	<LD	<LD	<LD	<LD	< LD
C_{32}-17α,21β Hopano (22S)	<LD	<LD	<LD	<LD	<LD	<LD	<LD	<LD	<LD	<LD	< LD
C_{32}-17α,21β Hopano (22R)	<LD	<LD	<LD	<LD	<LD	<LD	<LD	<LD	<LD	<LD	< LD

<LD: Abaixo do limite de detecção.